

UNCLASSIFIED

AD 4 6 3 0 7 8

DEFENSE DOCUMENTATION CENTER

FOR

SCIENTIFIC AND TECHNICAL INFORMATION

CAMERON STATION ALEXANDRIA, VIRGINIA



UNCLASSIFIED

NOTICE: When government or other drawings, specifications or other data are used for any purpose other than in connection with a definitely related government procurement operation, the U. S. Government thereby incurs no responsibility, nor any obligation whatsoever; and the fact that the Government may have formulated, furnished, or in any way supplied the said drawings, specifications, or other data is not to be regarded by implication or otherwise as in any manner licensing the holder or any other person or corporation, or conveying any rights or permission to manufacture, use or sell any patented invention that may in any way be related thereto.

AD No. 463078

DDC FILE COPY

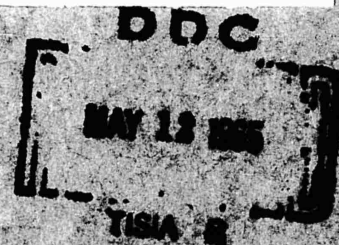
ANOMALY SELECTION FOR DEFLECTION INTERPOLATION
PART II: PRACTICAL APPLICATION



By
W. E. STRANGE and G. P. WOOLLARD

4 6 3 0 7 8

FINAL REPORT: PART II



Prepared for
AERONAUTICAL CHART AND INFORMATION CENTER
UNITED STATES AIR FORCE
ST. LOUIS, MISSOURI
CONTRACT AF23(601)-4009

nm

HAWAII INSTITUTE OF GEOPHYSICS
UNIVERSITY OF HAWAII



⑤ Hawaii Inst. of Geophysics,
Honolulu.

⑭ Rept. no.
HIG-64-13 - Pt. 12

①
ANOMALY SELECTION FOR DEFLECTION INTERPOLATION.
PART II. PRACTICAL APPLICATION.

⑩ by W. E. STRANGE and G. P. WOOLLARD.

⑪ Jul. 1964,

① FINAL REPORT, ~~SECRET~~

Prepared for

~~Aeronautical Chart and Information Center~~
~~United States Air Force~~
~~St. Louis, Missouri~~
⑮ Contract AF23(601) 4009

Approved by Director

George V. Woollard

Date: 3 August 1964

MB

ERRATA

Page 18 - last line, for $-.665''$ read $-.814''$

Page 26 - line 20, for $5.85''$ read $-5.85''$

Page 27 - line 19, for $+.606''$ read $+.820''$

Page 30 - line 4, for $\eta_f'' = -2.91'' \pm .5$ read $\eta_f'' = -2.94'' \pm .5$

Appendix page 2 - S X COS line, column 33, for 10277 read 102771

Appendix page 6 - S X COS line, column 27, for -9222 read -13146

Appendix page 22 - line 2, for -282.09 read 282.09

Appendix page 26 - line 1, for -135.33 read 135.33

(78)

ABSTRACT

Part I showed that (a) the type of anomaly was not critical in computing deflection of the vertical if the Molodenski theory was used and complete gravity knowledge existed, (b) what was critical was extrapolation of gravity values between observation points, (c) the complete Bouguer anomaly with geologic corrections provided the anomaly which allowed the most reliable extrapolations, and (d) the normal complete Bouguer anomaly provided the most readily derived values for computation of deflections. In this part of the final report, Part II, the procedure outlined in Part I is applied to the problem of interpolation of deflections of the vertical.

↓
In the Test Phase ^{utilized} ~~of the contract~~ three astro-geodetic deflection stations in the Rocky Mountain area of the western United States, ~~were~~ ^{utilized}. These were deflection stations 102, 105, and 116 from USC&GS Special Publication No. 229. Using the adopted procedure, the ~~X~~ deflection component was interpolated between stations 105 and 116 to obtain an interpolated ~~X~~ ^{X_i} value at station 102. A comparison of this interpolated ~~X~~ ^{X_i} value with the astro-geodetic ~~X~~ ^{X_a} value showed that the two differed by only .22". Since the accuracy of the astro-geodetic values probably do not exceed $\pm .2''$, the results were considered highly satisfactory.

^{pursued}
In the Application Phase ~~of the contract~~, deflection interpolation ~~was carried out~~ in an area in the Alps chosen by ACIC. In this case three deflection stations were chosen from a deflection of the vertical map provided by ACIC. These were designated stations 1, 2, and 3 for convenience. Using the adopted procedure, the ~~X~~ ^{X_i} deflection component was interpolated between stations 1 and 3 to obtain a value at station 2. As there were no individual deflection values given, the

→ to p ①

Handwritten: \downarrow T p (A)

Handwritten: (B)

astro-geodetic deflections were estimated from a η deflection component contour map with a 2.50" contour interval. Because of the manner of obtaining the astro-geodetic deflections, they are considered to have an accuracy of the order of $\pm .5''$.

For this reason the difference between the computed and observed η deflection components, $.59''$, has an uncertainty of $\pm 1.0''$. Since the difference again lies within the range of error inherent in the data the results are considered entirely satisfactory.



TABLE OF CONTENTS

Section 1 - General Comments	1
Section 2 - Test Phase - Method of Procedure	9
Section 3 - Test Phase - Results	15
Section 4 - Application Phase - Method of Procedure	22
Section 5 - Application Phase - Results	27
Section 6 - Summary and Conclusions	32
Bibliography	36

APPENDIX

Explanation of Tables	
Table 1 - Station 102 - Bouguer Correction and Bouguer Anomaly Components - Rice Rings 22 - 37	A-1
Table 2 - Station 105 - Bouguer Correction and Bouguer Anomaly Components - Rice Rings 22 - 37	A-3
Table 3 - Station 116 - Bouguer Correction and Bouguer Anomaly Components - Rice Rings 22 - 37	A-5
Table 4 - Station 102 - Bouguer Correction Component - Rice Rings 14 - 21	A-7
Table 5 - Station 116 - Bouguer Correction Component - Rice Rings 14 - 21	A-9
Table 6 - Station 116 - $\Delta\theta_p$ Correction - Rings A, B, and C	A-11
Table 7 - Station 116 - $\Delta\theta_p$ Correction - Rings D, E, and F	A-13
Table 8 - Station 1 - Bouguer Correction Component - Rice Rings 22 - 36	A-15
Table 9 - Station 2 - Bouguer Correction Component - Rice Rings 22 - 36	A-17
Table 10 - Station 3 - Bouguer Correction Component - Rice Rings 22 - 36	A-19
Table 11 - Station 1 - Bouguer Anomaly Component - Rice Rings 22 - 36	A-21
Table 12 - Station 2 - Bouguer Anomaly Component - Rice Rings 22 - 36	A-23
Table 13 - Station 3 - Bouguer Anomaly Component - Rice Rings 22 - 36	A-25
Table 14 - Station 2 - Bouguer Correction Component - Rice Rings 15 - 21	A-27

SECTION 1

GENERAL COMMENTS

In Part 1 of the final report on work completed under contract AF23(601)-4009 the final formula for deflection of the vertical computation was given as

$$\varphi_g = \frac{-R}{4\pi\gamma_Q} \int_s (\Delta g' + 2\pi k \sigma h) \frac{dS}{d\psi} (\psi) \frac{d\psi}{d\theta} dw + \Delta\theta_p \quad (1-1)$$

where φ_g is the gravimetric deflection in the angular direction θ

R = mean radius of the earth

γ_Q = theoretical gravity at deflection station

$\Delta g'$ = complete Bouguer anomaly

k = universal gravitational constant

σ = density used in computing Bouguer anomalies

h = elevation of surface

$S(\psi)$ = Stokes function

ψ = central angle between deflection station and incremental surface element dw

$\Delta\theta_p$ = correction factor dependent on elevation near deflection station

$$dw = \sin \psi d\psi dA$$

A = azimuth angle from computation point

The formula for $\Delta\theta_p$ can be stated

$$\Delta\theta_p = \frac{-k\sigma}{\gamma_Q} \int_s \left(\frac{1}{2} \frac{h^3}{r^3} - \frac{3}{8} \frac{h^5}{r^5} \right) \cos \frac{\psi}{2} \cos(r_o, l) dr dA \quad (1-2)$$

where r = distance from deflection station to incremental surface element, $\cos(r_o, l)$ = angle between the direction in which the deflection is being computed and direction of the surface element, dw .

$\bar{h} = \bar{h} - \bar{h}_o$ = elevation difference between station and surface element

The aim in the Test and Application Phases of the contract was

to test formulae (1-1) and (1-2) in making interpolations of deflections of the vertical. In making the test deflection of the vertical interpolations, optimum use was made of both astro-geodetic and gravimetric information for computing a deflection at a point lying between stations where astro-geodetic deflections were available. If one had complete knowledge of the gravity field and carried out the integrals of (1-1) and (1-2) around the world to determine a gravimetric deflection at an astro-geodetic station, the gravimetric deflection would be identical to the astro-geodetic deflection -- assuming the astro-geodetic deflection was accurate and was referred to the same reference ellipsoid as that used in computing the gravity anomalies. The major part of the deflection components at a station is due to the values of the integrated quantities of equations (1-1) and (1-2) within a short distance of the deflection station. This contribution of the near area varies irregularly from point to point. The effect of the gravity field at greater distances, on the other hand, has less effect on the deflection and is a smoothly varying function.

If we label the astro-geodetic deflection as φ_a and the gravimetric deflection as φ_g we can write

$$\varphi_a = \varphi_g = \varphi_{g_n} + \varphi_{g_f} \quad (1-3)$$

where φ_{g_n} represents the part of the gravimetric deflection obtained by integration of (1-1) and (1-2) over the area near the deflection station, and lying within a circle having a radius r_1 described about the station,

and φ_{g_f} represents the part of the gravimetric deflection obtained by integration of (1-1) and (1-2) over the area lying at a distance greater than r_1 from the deflection station. The value of r_1 will depend upon how much area it is desirable to retain in the "near" part of the deflection, φ_{g_n} . In general, the value of r_1 will

be controlled by the smoothness of the gravity field and the distance over which deflection interpolation is to be carried out.

To obtain a deflection at an intermediate station lying between two astro-geodetic stations, φ_{g_n} is computed at each astro-geodetic station by numerically evaluating the integrals of (1-1) and (1-2) between zero and r_1 .

Then at each astro-geodetic deflection station we can compute

$$\varphi_f' = \varphi_a - \varphi_{g_n} \quad (1-4)$$

Since φ_f' is a smoothly varying function, one can compute the value of φ_f' at the intermediate station by linear interpolation between the two astro-geodetic stations. Then φ_{g_n} is computed at the intermediate station in the same way as it was at the astro-geodetic stations, added to the interpolated φ_f' value, and a complete deflection of the vertical which we shall designate, φ_{ga} , obtained.

In many cases the orientation and origin of the ellipsoid to which the astro-geodetic deflections are referenced differs from the International Ellipsoid to which the gravity values are referenced. So long as one desires the intermediate deflection to be referenced to the same ellipsoid as the astro-geodetic deflections, this presents no problem in carrying out the interpolation. In the case of a difference in reference ellipsoid, equation (1-3) becomes

$$\varphi_a = \varphi_g + \Delta\varphi_e = \varphi_{g_n} + \varphi_{g_f} + \Delta\varphi_e \quad (1-5)$$

where $\Delta\varphi_e$ represents the angle between the normals to the two ellipsoids at the point. Then at each astro-geodetic station we have

$$\varphi_f'' = \varphi_a - \varphi_{g_n} = \varphi_f' + \Delta\varphi_e \quad (1-6)$$

Since $\Delta\varphi_e$ is a smoothly varying function, we can interpolate to get φ_f'' at the intermediate station and then compute φ_{g_n} there to again

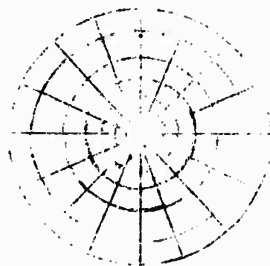
arrive at a φ_{g_a} value at the intermediate station which is referenced to the astro-geodetic ellipsoid.

Rice has developed a method of numerically computing the value of an integral of the form

$$\frac{-R}{4\pi\gamma_Q} \int_0^{360} \int_0^\psi 1 F \frac{dS(\psi)}{d\psi} \frac{d\psi}{d\theta} \sin \psi d\psi dA \quad (1-7)$$

where F can be any type of gravity anomaly. This method can be used to evaluate the integral of equation (1-1).

In Rice's method a template such as indicated schematically below is used.



The template is so set up that for each of the compartments beyond the central circle one need only multiply the average gravity anomaly in mgls of that compartment by the cosine of the angle between the direction of the center of that compartment and the direction in which the deflection is being computed and then by .001 to give the deflection contribution of that compartment in seconds.

The effect of the central circle is then computed by using values of gravity on the circle's perimeter to estimate the gravity gradient within the circle. The details of the template and central circle computation as used by Rice are given in Heiskanen and Vening Meinesz (1958) and are well known to most geodesists. They will not be repeated here.

In the present problem the Rice template is used twice to compute the effect of the area outside the central circle.

First the integral

$$\frac{-R}{4\pi\gamma_Q} \int_0^{360} \int_{\psi_0}^{\psi_1} \Delta g' \frac{dS(\psi)}{d\psi} \frac{d\psi}{d\theta} \sin \psi d\psi dA \quad (1-8)$$

is evaluated using Rice's template with average values of $\Delta g'$ being picked for each compartment.

The integral

$$\frac{-R}{4\pi\gamma_Q} \int_0^{360} \int_{\psi_0}^{\psi_1} 2\pi k\sigma h \frac{dS(\psi)}{d\psi} \frac{d\psi}{d\theta} \sin \psi d\psi dA \quad (1-9)$$

is then evaluated using Rice's template in the following manner. A normal template calculation is carried out using the average elevation for each compartment rather than a gravity anomaly. The final result is then multiplied by $2\pi k\sigma$ to convert from feet to mgls and thus give the correct deflection contribution of the integral.

A central circle calculation is then carried out to determine the contribution of the central circle to each of the integrals of (1-8) and (1-9).

As shown in Part I of this final report, for computation of the quantity $\Delta \theta_p$, one may sum the effect of a number of annular compartments, either the compartments of the Rice template or others. The effect of a single compartment is given by

$$\Delta(\Delta \theta_p) = \frac{k\sigma}{\gamma_Q} \Delta A \cos(r_o, 1) \left\{ \frac{h^3}{4} \left(\frac{1}{r_1^2} - \frac{1}{r_2^2} \right) - \frac{3h^5}{32} \left(\frac{1}{r_1^4} - \frac{1}{r_2^4} \right) \right\} \quad (1-10)$$

where ΔA is the angular width of the compartment

and r_1 and r_2 are the inner and outer radii of the compartment.

One could, of course, establish any values one desired for ΔA and for the various radii increments. If, for example, we use

$\Delta A = 15^\circ = .2617$ radians, then equation (1-10) becomes

$$\Delta(\Delta\theta)_p = +.6947 \times 10^{-2} \cos(r_o, 1) \bar{h}^3 \left(\frac{1}{r_1^2} - \frac{1}{r_2^2} \right) - 2.42 \times 10^{-6} \cos(r_o, 1) \bar{h}^5 \left(\frac{1}{r_1^4} - \frac{1}{r_2^4} \right) \quad (1-11)$$

where \bar{h} is given in units of thousands of feet and r_1 and r_2 are given in km. If \bar{h} is in km the constants in equation (1-11) become

$$+ .2117 \times 10^{-2} \text{ and } -.8186 \times 10^{-5}$$

We shall call the term containing \bar{h}^3 the secondary correction and the term containing \bar{h}^5 the tertiary correction. Let us see how these quantities vary with r . We can write the secondary correction as

$$+.6947 \times 10^{-2} \cos(r_o, 1) \bar{h}^3 \left(\frac{1}{r_1^2} - \frac{1}{r_2^2} \right) = F(r_1, r_2) \cos(r_o, 1) \bar{h}^3$$

where $F_1(r_1, r_2) = .6947 \times 10^{-2} \left(\frac{1}{r_1^2} - \frac{1}{r_2^2} \right)$ (1-12)

Then the following table gives the value of $F(r_1, r_2)$ for various values of r_1 and r_2 in kms where \bar{h} must be given in units of thousands of feet.

r_1	r_2	$F(r_1, r_2)$
km	km	
.2	.5	14.5337×10^{-2}
.5	.75	1.5436×10^{-2}
.75	1.1	$.6614 \times 10^{-2}$
1.1	1.55	$.2841 \times 10^{-2}$
1.55	2.13	$.1452 \times 10^{-2}$
2.13	3.07	$.0709 \times 10^{-2}$
3.07	4.32	$.0520 \times 10^{-2}$

The tertiary correction can be written

$$-2.4202 \times 10^{-6} \cos(r_o, 1) \bar{h}^5 \left(\frac{1}{r_1^4} - \frac{1}{r_2^4} \right) = G(r_1, r_2) \cos(r_o, 1) \bar{h}^5$$

$$\text{where } G(r_1, r_2) = -2.4202 \times 10^{-6} \left(\frac{1}{r_1^4} - \frac{1}{r_2^4} \right) \quad (1-13)$$

Then the values of $G(r_1, r_2)$ for various r_1, r_2 values are given below where again it is assumed r_1 and r_2 are in kms and h in thousands of feet.

r_1 km	r_2 km	$G(r_1, r_2)$
.2	.5	$.1474 \times 10^{-2}$
.5	.75	$.0031 \times 10^{-2}$
.75	1.1	$.0006 \times 10^{-2}$
1.1	1.55	$.00012 \times 10^{-2}$

The above tables show that the secondary correction can be computed sufficiently accurately by integrating only over an area within 5 km of the deflection station in the normal case. The tertiary correction normally need only be integrated over an area within 1 km of the deflection station. Indeed, unless the elevation changes involved are rather large, the $\Delta\theta_p$ correction can be ignored.

The solution given in equation (1-10), as was the case for the Stokes' equation, cannot be used within a small central circle around the deflection station. No attempt was made to obtain a central ring solution for equation (1-10). It was felt that the assumption that the area within .2 km (about 600 ft.) of a deflection station is sufficiently level to introduce no significant error was reasonable.

The first question which naturally arises in carrying out the deflection interpolation is the question of how far it is necessary to carry out the numerical integrations of equations (1-8) and (1-9) so that the φ'_f or φ''_f value obtained can be linearly interpolated between the astro-geodetic stations. The answer to this question depends of course upon the distance between astro-geodetic stations. Molodensky et al (1960) suggest that as a minimum the integration be carried out to a distance from each station equal to the separation of the astro-geodetic stations. Of course theoretically the further the integration

is carried out the more nearly linear will be the interpolated quantity. In both the Test and Application Phases of this study the integration was carried out to a distance approximately equal to the separation of the astro-geodetic deflection stations. This appeared to be adequate to obtain an answer whose accuracy was consistent with the accuracy of the gravity and deflection data used in the computations and comparisons. Where modern astro-geodetic deflections are available with an accuracy of .1" or better and a reasonably dense net of high quality gravity stations are available, it might be desirable to extend the integration over a circular area whose radius was about twice the distance between deflection stations in order to aim at an interpolation accuracy of between .1" and .2".

In evaluating the integrals of equations (1-8) and (1-9) using the Rice template and inner circle method, it is always necessary to decide the radius of the inner circle. Such a decision must be made in each case on the basis of the smoothness of the variation of the quantity being integrated near the deflection station.

SECTION 2

TEST PHASE - METHOD OF PROCEDURE

In order to test the accuracy of the selected deflection interpolation procedure, application of the theory to actual data was undertaken. Three astro-geodetic deflection stations were selected in the western United States to use in carrying out the test. These were deflection stations 102, 105, and 116 from USC&GS Special Publication No. 229 (1941).

The test was carried out as follows: the meridional deflection, ξ , was considered to be known at stations 116 and 105 and the interpolation procedure performed to obtain a computed deflection at station 102. This computed deflection was then compared with the astro-geodetic deflection at station 102 as a measure of the accuracy of the deflection interpolation procedure.

Steps followed in deriving the interpolated deflection values, were as follows:

1. The area within 65.9 km of each deflection station (through Rice Ring 37) was chosen as the near area over which equations (1-1) and (1-2) were to be numerically integrated to obtain ξ_{3n} values.

2. For the area between 4.32 km and 65.9 km, elevation contour maps, scale 1:250,000, were used to obtain average elevations for the compartments of a Rice template. These average elevations were used to evaluate the integral of equation (1-9) in this region.

3. To obtain the summation of (1-9) over the area within 4.32 km of the stations, the following procedure was used. For deflection stations 116 and 102, an elevation map whose scale was 1:62,500 was used with a Rice template to pick average elevations for evaluating the integral between 1.099 km and 4.32 km from the deflection station. The Rice inner circle procedure employing the three gradient method was used to compute the effect of the area within 1.099 km of these

two stations. In the case of deflection station 105, an inner circle procedure employing the single gradient method was used for the entire area within 4.32 km of the station since the topography was relatively smooth near this station.

4. Using the elevation map of scale 1:62,500, average elevations were determined for use in computing $\Delta\theta_p$ at station 116 employing equation (1-10). The details of the size of sectors over which averaging was carried out are discussed with the results. Preliminary calculations showed that the $\Delta\theta_p$ correction would be negligible at stations 105 and 102, thus it was not computed for these stations.

5. Simple Bouguer anomalies were plotted on a transparent paper overlay for the 1:250,000 elevation contour maps. Terrain corrections were then computed using the procedure developed under contract AF 23 (601)-3789 and complete Bouguer anomalies obtained.

6. Using geophysical and geologic information to control the interpolation between observation points, a Complete Bouguer anomaly contour map was prepared on the scale 1:250,000.

7. Using a Rice template, average anomalies for compartments were determined for the area between 4.32 km and 65.9 km and used to evaluate the integral of equation (1-8) in this area. The Rice inner ring procedure was used to evaluate (1-8) over the area within 4.32 km of each station.

8. The final computation of the part of the meridional deflection, component, ξ_{g_n} due to the gravity field of the near area (within 65.9 km of a station) was made for each station using the results obtained in the preceding steps.

9. At stations 116 and 105, the deflection contribution of the near area was subtracted from the astro-geodetic deflections. The result,

ξ_f'' was the deflection contribution of the gravity field of the area beyond 65.9 km plus the effect of the differences between the gravimetric and astro-geodetic ellipsoids.

10. Using a simple linear interpolation between Stations 116 and 105, the value ξ_f'' was determined at Station 102. This interpolated value was then added to the previously computed deflection effect of the near area ξ_{gn} at Station 102 to give a computed meridonal deflection component at Station 102. This was then compared with the astro-geodetic value, ξ_a , to test the accuracy of the interpolation procedure.

The above steps give in outline form the manner in which the deflection interpolation procedure was carried out for the Test Phase of the Contract. The paragraphs below give additional details concerning the computations indicated in the above outline.

Elevation Contour Map Selection

The first step in evaluating the integral of equation (1-9) was the selection of elevation contour maps from which average elevations could be determined for the template compartments. The choice of map scale was controlled by the amount and quality of the gravity data present. An elevation contour map should be chosen which would allow the average elevations of the compartments of the template to be determined with an accuracy such that the quantities $2\pi k\sigma h$ computed from them would be about equal in accuracy to the average Complete Bouguer anomalies determined for the same compartments. It was felt that the compartment averages of Complete Bouguer anomaly could be determined to an accuracy of about ± 3 mgls. Thus an elevation accuracy of about ± 100 ft. was desired. For the area outside Rice ring 21 (outer radius 4.32 km), the 1:250,000 series of Transverse Mercator Projection maps prepared by the Army Map Service and sold by the U. S. Geological Survey was considered adequate. For the area within 4.32 km of a deflection station, a larger

scale map was desired. For the present problem the 1:62,500 special topographic quadrangle maps of the U. S. Geological Survey were chosen.

Transverse Mercator Projection maps were used throughout the computations. Transverse Mercator Projection maps cannot, of course, be used in carrying out world-wide computations, but they are accurate enough to be used for interpolation computations where only areas of 1 to 2 degrees square need be used in the integration.

The manner in which the average elevations of the compartments were determined varied depending upon the size of the compartment and the ruggedness of the topography. For the smallest compartments and in level areas the average compartment elevation was estimated directly by visual inspection. For the larger compartments, particularly where the topography was rugged, the compartment was divided into a number of subsections -- up to nine subsections in the most extreme case. The average elevations of these subsections were then determined and themselves averaged to obtain the average elevation for a compartment.

Preparation of Bouguer Anomaly Map

To obtain the Complete Bouguer anomaly contour map necessary to use for determination of compartment averages utilizing a Rice template, the following procedure was chosen. The simple Bouguer anomalies were first plotted on a transparent tracing paper overlay on the 1:250,000 Transverse Mercator elevation contour maps. Then, using a procedure developed under contract AF 23(601)-3789, terrain corrections were made at all stations where it was felt that the correction exceed 1.5 mgls. The terrain correction procedure is not described here as it will be found in the final report to contract AF 23(601)-3789. Once the complete Bouguer anomalies had been computed and plotted, the contouring of the complete Bouguer anomaly map was undertaken. It was at this point that geologic and geophysical knowledge were interjected. The geologic

and geophysical knowledge was used to control the interpolation (i.e., contouring) between points of observation. The primary utilization of geologic knowledge was in contouring the gravity data in the Rocky Mountain Front Range of Colorado and in the area of transition from the Denver-Julesburg Basin to the Front Range Uplift. To gain insight into the form the gravity field should have in passing from the basin to the uplift, a geologic density section based on available geologic knowledge was prepared and a gravitational profile computed. Utilizing these results, the available gravity data, and knowledge of the location of the fault boundary between the basin and the uplift, the contouring in this area was carried out. On the western side of the Front Range uplift not enough information was found to justify numerical computation of the geologic effect. The best that could be done was to utilize the available geologic knowledge of structural relations, approximate thickness of sediments, and location of recent Cenozoic intrusives to control the contouring. The geologic control utilized in the contouring process although largely non-quantitative rather than quantitative proved highly successful as witnessed by the results obtained.

SECTION 3

TEST PHASE - RESULTS

In Tables 1 through 3 of the Appendix are presented the average Complete Bouguer anomalies and average elevations for each compartment of Rice circles 22 through 37 for the three deflection stations used in the Test Phase. In each case the results for similar compartments of each ring were summed and each sum multiplied by the appropriate cosine. The sum times cosine results were in turn summed to give a single result for each of the two quantities at each station. The final Complete Bouguer anomaly result at each station was multiplied by .001 to give the Complete Bouguer anomaly component in seconds of arc. The final average elevation result was multiplied first by .03406 to convert to mgls and then by .001 to obtain the Bouguer correction contribution to the ξ_{g_n} deflection component. The results are listed below.

Station 116	
Bouguer Correction Component	+ 1.290"
Complete Bouguer Anomaly Component	+ .829"
Station 105	
Bouguer Correction Component	- 3.659"
Complete Bouguer Anomaly Component	- .084"
Station 102	
Bouguer Correction Component	- 3.450"
Complete Bouguer Anomaly Component	+ 2.012"

For the circular area between the deflection stations and Rice ring 22 (0 to 4.32 km) the effects of the two components were computed using such combinations of template summation and central circle computation as were considered necessary to obtain adequate accuracy.

The Complete Bouguer Anomaly Component was computed at each station by a Rice central circle computation. The results of these computations are given below.

At Stations 116 and 105 the Complete Bouguer anomaly contour lines run almost directly north-south. Thus at these stations the Complete Bouguer anomaly component for the central circle was found to be zero.

For Station 102, the single gradient method (See Heiskanen and Vening Meinesz, 1958) was used to get the Complete Bouguer anomaly component of the inner ring. Using the formula

$$\Delta \xi = .105 r_o \frac{(\Delta g_s - \Delta g_n)}{\Delta x}$$

and the values $r_o = 4.32$ km

$$\Delta x = 8.64 \text{ km} \quad \Delta g_s = - 219 \text{ mgls} \quad \Delta g_n = - 227 \text{ mgls}$$

we get
$$\Delta \xi = .105 \frac{(- 219 + 227)}{2} = 0.42''$$

The elevation contour map which had to be integrated to obtain the Bouguer correction component had a more complex contour pattern than the Complete Bouguer anomaly component and required the use of a combination of template and central circle computation to evaluate the effect of the area within 4.32 km of each station. For stations 116 and 102, 1:62,500 scale maps were used with a Rice Template to obtain the Bouguer correction component for Rice zones 14 through 21. The results are given in Tables 4 and 5 of the Appendix. The deflection contributions resulting from this template summation were

$$\text{Station 116} \quad + 1.50''$$

$$\text{Station 102} \quad - .32''$$

The small inner circle of 1.1 km radius was evaluated at each of these stations using a three gradient method. The results given below were computed using the formula

$$\Delta \xi'' = 0.105 r_o \frac{(\Delta g_s - \Delta g_n)}{\Delta x} = 0.003576 r_o \frac{(E_s - E_n)}{\Delta x}$$

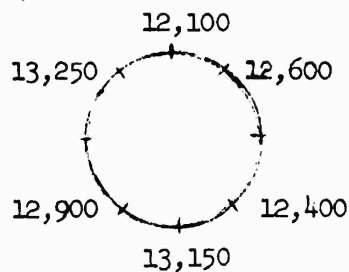
$$E_s = \text{southward elevation}$$

$$E_n = \text{northward elevation}$$

$$\Delta \xi'' = \text{deflection contribution of central circle}$$

Station 116

$$r_o = 1.1 \text{ km}$$



FOR CENTRAL INTERVAL

$$E_s - E_n = 13,150 - 12,100 = 1050$$

$$\Delta X = 2.2 \text{ km}$$

$$\text{and } \Delta \xi_c = (0.105) (.03406) \left(\frac{1050}{2} \right) = (0.105)(.03406)(525)$$

$$\Delta \xi_c = (55.12)(.03406) = + 1.88''$$

FOR RIGHT INTERVAL

$$E_s - E_n = (12,400 - 12,600) = - 200$$

$$\Delta X = 1.5556$$

$$\Delta \xi_R = (0.105)(1.1) \frac{(.03406)(- 200)}{1.5556} = - .506''$$

FOR LEFT INTERVAL

$$E_s - E_n = (12,900 - 13,250) = - 350$$

$$\Delta X = 1.5556$$

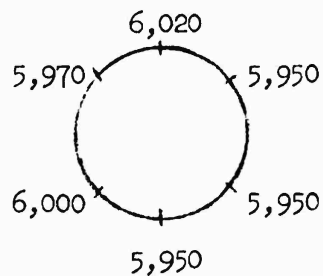
$$\Delta \xi_L = (0.105) \frac{(1.1)(.03406)(- 350)}{1.5556} = - .885''$$

$$\Delta \xi \text{ AVERAGE} = \frac{1}{2} \left(\Delta \xi_c + \frac{\Delta \xi_R + \Delta \xi_L}{2} \right) = \frac{1}{2} \left(1.88 - \frac{(.506 + .885)}{2} \right)$$

$$\Delta \xi \text{ AVERAGE} = \frac{1}{2} (1.88 - .70) = \frac{1}{2} (1.18) = .59''$$

Station 102

$$r_o = 1.1 \text{ km}$$



FOR CENTRAL INTERVAL

$$E_s - E_n = (5950 - 6020) = - 70$$

$$\Delta X = 2.2 \text{ km}$$

$$\Delta \xi''_c = (0.105)(1.1)(.03406) \frac{(- 70)}{2.2}$$

$$\Delta \xi''_c = - .125$$

FOR RIGHT INTERVAL

$$E_s - E_n = 0$$

$$\Delta \xi''_R = 0$$

FOR LEFT INTERVAL

$$E_s - E_n = (5970 - 6000) = - 30$$

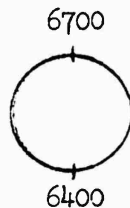
$$\Delta X = 1.5556$$

$$\Delta \xi''_L = (0.105)(1.1) \frac{(.03406)(- 30)}{1.5556} = - .076$$

$$\Delta \xi \text{ AVERAGE} = \frac{1}{2} (\Delta \xi_c = \frac{\Delta \xi_R + \Delta \xi_L}{2}) = \frac{1}{2} (- .125 - \frac{(0 + .076)}{2})$$

$$\Delta \xi \text{ AVERAGE} = \frac{1}{2} (- .125 - .038) = \frac{1}{2} (- .163) = - .081$$

For Station 105 the Bouguer correction component was computed using the single gradient method for the area within 4.32 km of the deflection station since the topography varied in a linear manner near this station. The results are given below.



$$r_o = 4.32 \text{ km}$$

$$\Delta X = 8.64 \text{ km}$$

$$\text{Then } \Delta \xi'' = (.105)(.03406) \frac{(6400 - 6700)}{2}$$

$$\Delta \xi'' = - (.105)(.03406)(150)$$

$$\Delta \xi'' = - (.003576)(150)$$

$$\Delta \xi'' = - .536''$$

As pointed out in Section 1, very large changes in elevation are required very near a station in order for the correction factor $\Delta\theta_p$ to be sufficiently large to require computation. For this reason only at Station 116 did the component $\Delta\theta_p$ have a significant contribution to the final deflection. For this station $\Delta\theta_p$ was computed using equation (1-2) and a template with the radii of the rings being as follows:

	<u>Inner radius</u>	<u>Outer radius</u>
Ring A	.2 km	.5 km
Ring B	.5 km	.75 km
Ring C	.75 km	1.1 km
Ring D	1.1 km	2.0 km
Ring E	2.0 km	3.0 km
Ring F	3.0 km	4.0 km

Rings A, B, and C were divided into annular sections of 10 degrees as in the Rice template. Rings D, E, and F were divided into annular sections of 15 degrees. The area within .2 km was assumed to have zero contribution.

As stated in Part I of the final report, average elevations obtained using a Rice template would normally be used so that average elevation determinations already available from determination of the Bouguer correction component could be utilized. In the present case, the computation of the $\Delta\theta_p$ component at Station 116 had already been accomplished using the template divisions described above before it was decided that the results of the Rice template computations would have been satisfactory. Thus, this solution was retained since recomputing would not have contributed to any increase in accuracy. The results of the $\Delta\theta_p$ computations are given in Tables 6 and 7 in the Appendix. The contribution of this term to the deflection at Station 116 was - .665".

With the results given above we are now in position to carry out the deflection interpolation. Below is given a summary of the above results at each station.

Station 116

Bouguer Correction Component (4.32 km to 65.9 km)	+ 1.290"
Bouguer Correction Component (1.099 km to 4.32 km)	+ 1.500"
Bouguer Correction Component (0 to 1.099 km)	+ <u>.590"</u>
TOTAL Bouguer Correction Component	+ 3.380"
Complete Bouguer Anomaly Component (4.32 km to 65.9 km)	+ .829"
Complete Bouguer Anomaly Component (0 to 4.32 km)	<u>.000"</u>
TOTAL Complete Bouguer Anomaly Component	+ .829"
$\Delta\theta_p$ Component	<u>- .814"</u>
TOTAL value of ξ_{gn}	+ 3.395"

Station 105

Bouguer Correction Component (4.32 km to 65.9 km)	- 3.659"
Bouguer Correction Component (0 to 4.32 km)	- <u>.536"</u>
TOTAL Bouguer Correction Component	- 4.195"
Complete Bouguer Anomaly Component (4.32 km to 65.9 km)	- .084"
Complete Bouguer Anomaly Component (0 to 4.32 km)	<u>.000"</u>
TOTAL Complete Bouguer Anomaly Component	- .084"
$\Delta\theta_p$ Component	- <u>.000"</u>
TOTAL vlaue of ξ_n	- 4.279

Station 102

Bouguer Correction Component (4.32 km to 65.9 km)	- 3.450"
Bouguer Correction Component (1.099 km to 4.32 km)	- .320"
Bouguer Correction Component (0 to 1.099 km)	- <u>.081"</u>
TOTAL Bouguer Correction Component	- 3.851"

Complete Bouguer Anomaly Component (4.32 km to 65.9 km)	+ 2.012"
Complete Bouguer Anomaly Component (0 to 4.32 km)	+ .420"
TOTAL Complete Bouguer Anomaly Component	+ 2.432"
$\Delta \theta_p$ Component	.000"
TOTAL value of ξ_{gn}	- 1.419"

The computation of $\xi_{gf} + \Delta \xi_e$ gives the following results for the two stations, 116 and 105, at which astro-geodetic deflections were assumed known:

Station 116

Astro-geodetic deflection ξ_a	+ 1.35"
Effect of near region ξ_{gn}	+ 3.40"
$\xi_a - \xi_{gn} = \xi_{gf} + \Delta \xi_e$	- 2.05"

Station 105

Astro-geodetic deflection ξ_a	- 5.34"
Effect of near region ξ_{gn}	- 4.28"
$\xi_a - \xi_{gn} = \xi_{gf} + \Delta \xi_e$	- 1.06

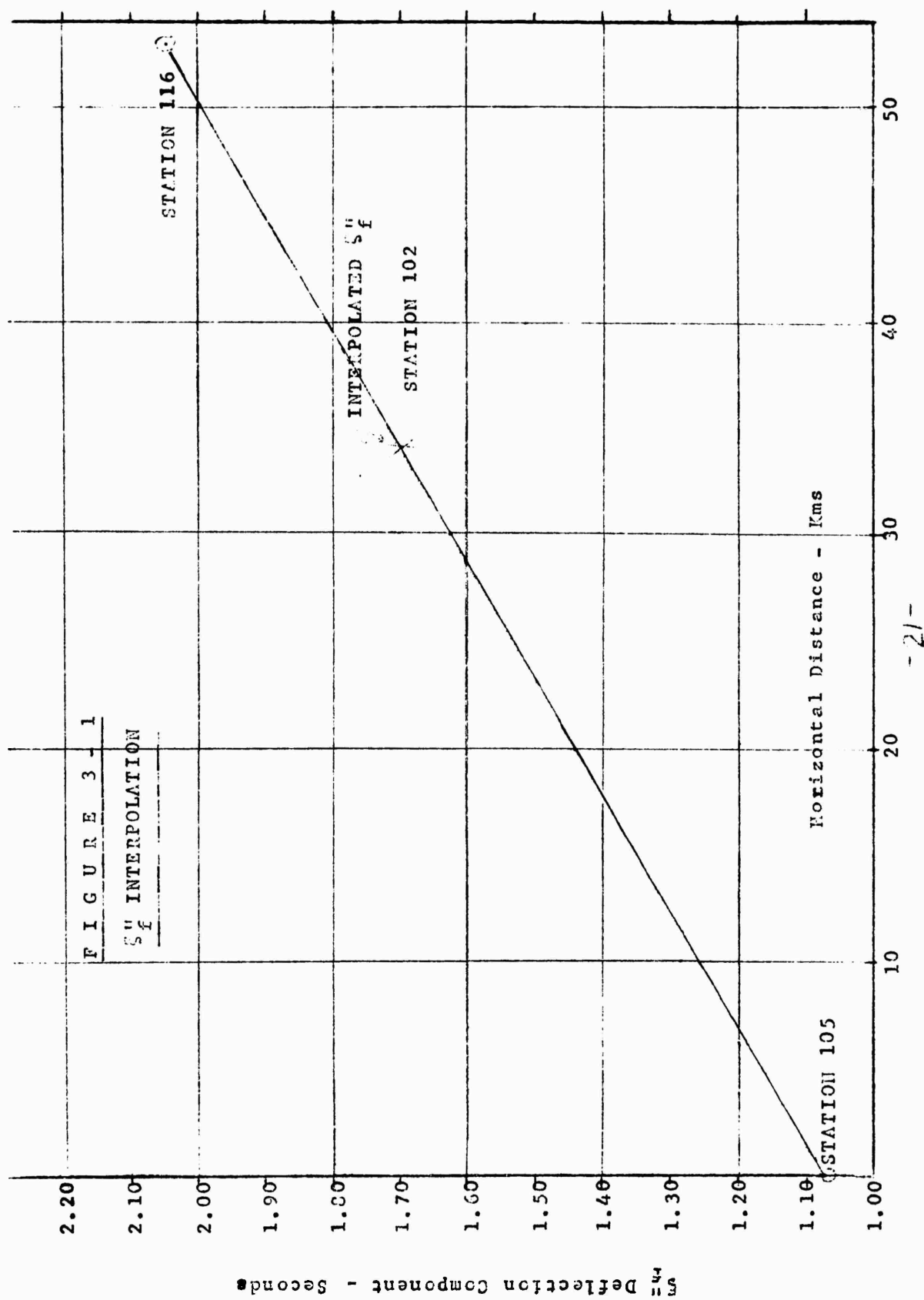
Figure 3-1 shows the linear interpolation carried out to obtain a value of $\xi_{gf} + \Delta \xi_e$ for Station 102. The value obtained for Station 102 is

$$\xi_{gf} + \Delta \xi_e = - 1.69$$

But the value of ξ_{gn} computed for Station 102 was - 1.42". Thus the interpolated deflection for Station 102 is

$$\xi_a = - 1.69" - 1.42" = - 3.11"$$

The astro-geodetic deflection for Station 102 is - 2.89". Thus the interpolated deflection value and the observed deflection value differ only by .22".



SECTION 4

APPLICATION PHASE - METHOD OF PROCEDURE

In order to test the applicability of the deflection interpolation procedure developed under this contract to general usage in all areas of the world the procedure was used to interpolate deflections of the vertical in the European Alps. Gravity data and astro-geodetic deflections for this phase of the study were provided by ACIC. The gravity data consisted of 2000 gravity stations located over eleven $1^{\circ} \times 1^{\circ}$ squares in the European Alps. The astro-geodetic deflection stations were selected in conjunction with ACIC from stations shown on a contour map of η deflection components. These astro-geodetic stations were for convenience labeled #1, #2, and #3. Their location as determined by scaling from the contour maps were as follows:

Station #1	Lat. $47^{\circ} 22.5'N$	Long. $8^{\circ} 40.5'E$
Station #2	Lat. $47^{\circ} 22.5'N$	Long. $9^{\circ} 01.5'E$
Station #3	Lat. $47^{\circ} 22.5'N$	Long. $9^{\circ} 39.0'E$

Because of the large number of gravity stations and the excellent elevation data available it was hoped that the application of the present deflection interpolation procedure in the Alpine area would provide an excellent test of the method. However, the test did not prove as conclusive as was first hoped. There were two primary reasons for this. First, the form in which the astro-geodetic information was available placed a limit on the extent to which the accuracy could be tested. The values of the astro-geodetic deflection components could be determined from the contour maps only to an accuracy of about $\pm .5''$. Thus it was only possible to determine if the accuracy of the interpolated deflection was within the range of the cumulative uncertainty which was approximately $\pm 1.0''$. Also, because of the scale of the deflection contour map,

1 inch = 70 km, uncertainty of about $\pm 1.0'$ exists in the location of the stations as scaled from these maps. This introduces uncertainties into the computed η_{gn} components which are estimated to be in the range of .1" to .3".

A second problem encountered was in the distribution and accuracy of the gravity data. It was originally anticipated that the 2000 stations would lie approximately within a $3^\circ \times 3^\circ$ square or nine $1^\circ \times 1^\circ$ squares. Instead the data was located within eleven $1^\circ \times 1^\circ$ squares. Moreover, nearly half the stations, about 900, were located within one $15' \times 15'$ square area. After plotting of the data and computation of the terrain corrections an attempt was made to contour the data. At this time, two more problems were encountered. First, it was found that at many stations there were two gravity anomaly values given which differed by 2.0 mgls. A check of latitude, longitude, and elevation data showed that this discrepancy evidently resulted from the listing of the same survey twice with different base values used for each listing. One set of values was chosen and the other set rejected on the basis of comparisons with other stations.

Second, it was found that in some places closely spaced stations differed by several tens of milligals. Also in certain areas where only a few stations occurred, it was found that contouring using the available data produced a gravity anomaly contour map which had no apparent relation to geology and, in fact, appeared to crosscut geologic structure. Such a gravity pattern appeared to be highly unlikely. The cause of the above discrepancies was traced to certain series of very old pre-1900 pendulum data. This data was in error by amounts up to 50 mgls. This series of stations was discarded and the contour map redrawn. However, because of the factors listed above, there were left available for contouring the complete Bouguer anomaly map even fewer useful data points

than had been available for the Test Phase.

The above factors although disappointing in one sense do tend to emphasize certain useful facts. Foremost is the fact that where observational data is suspect, the employment of geologic knowledge can lead to criteria for acceptance or rejection of the data. Second is the fact that even a very small amount of accurate data when judiciously handled will give reasonably good deflection results.

Since the details of procedure for the Application Phase of the contract were similar to those of the Test Phase they will not be brought out here. Certain special details do, however, merit mention.

The area used in computation of the η_{gn} components is somewhat smaller than would normally be used if precise answers were desired. That is, if one were attempting .1" accuracy with plentiful gravity data, integration should be carried out over several additional Rice rings than were used in the present case. Considering the accuracy of the astro-geodetic data, however, such an extension in the integration area would not be expected to yield any additional useful information in the present case. In fact, as a check, the integration was extended through an additional Rice ring (ring 37) after all the tables included in this report had been completed.

These extensions changed the actual values of η_{gn} by amounts in the range .1" to .2" and altered the interpolated η_f'' value by less than .1". This indicated that the range of change to be expected by extension of the area of integration was so small as to be of questionable meaning considering the sparse gravity control. In any case, the uncertainty in the astro-geodetic deflections precludes any meaningful interpretation of the effect of including the additional area on the accuracy of interpolated deflections.

The elevation contour maps used for the determination of average compartment elevation in areas beyond 4.32 km from deflection stations were Army Map Service 1:250,000 Transverse Mercator Projection maps, series 1959. For the area within 4.32 km of the deflection stations, German 1:50,000 scale elevation contour maps were used to estimate average elevations.

SECTION 5

APPLICATION PHASE - RESULTS

The results of the Application Phase of the Contract are outlined here with the various tables given in the Appendix.

The Bouguer Correction Component for all three stations was computed for the area between 4.32km and 55.66km using the 1:250,000 scale maps. The Complete Bouguer Anomaly Component was computed using the Complete Bouguer anomaly contour map prepared on the 1:250,000 scale. The average compartment elevation values used to compute the Bouguer correction component are given in Table 8, 9, and 10 in the Appendix. The average Complete Bouguer anomalies for the compartments are given in Tables 11, 12, and 13 of the Appendix.

The final results for the above summations between 4.32km and 55.66km at the three deflection stations are given below:

Station #1

Bouguer Correction Component	-2.34"
Complete Bouguer Anomaly Component	+2.47"

Station #2

Bouguer Correction Component	-1.62"
Complete Bouguer Anomaly Component	+1.87"

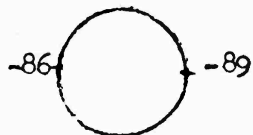
Station #3

Bouguer Correction Component	5.85"
Complete Bouguer Anomaly Component	+3.11"

For station #1 a three gradient computation was carried out for the Bouguer Correction Component and a single gradient computation for the Complete Bouguer Anomaly Component within the 4.32km radius central circle.

The results were:

Complete Bouguer Anomaly Component



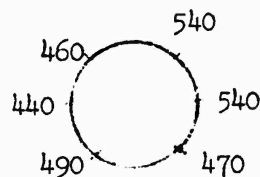
$$r_o = 4.32 \quad \Delta g_w = -86_m \quad \Delta g_e = -89$$

$$\Delta \eta'' = .0525 [(-86) - (-89)] = + .16''$$

Bouguer Correction Component

$$r_o = 4.32$$

central interval	$\Delta \eta'' = - .59''$
north interval	$\Delta \eta'' = - .67''$
south interval	$\Delta \eta'' = + .17''$
Average	$\Delta \eta'' = - .42''$



For station #2 a single gradient central circle computation was carried out to obtain the Complete Bouguer Anomaly Component of the inner circle. The Bouguer Correction Component was obtained by using a template summation between 1.304km and 4.32km and a three gradient central circle calculation for the area within 1.099km of the station. The average elevation results of the template calculation are given in Table 14 of the Appendix. The Bouguer Correction Component of the deflection for the area between 1.304km computed from these average elevations was + .606". The results of the two central circle computations were:

Complete Bouguer Anomaly Component

$$r_o = 4.32km \quad \Delta g_w = -101 \quad \Delta g_e = -102$$

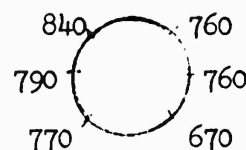
$$\Delta \eta'' = .0525 [-101 - (-102)]$$

$$\Delta \eta'' = .052''$$



Bouguer Correction Component

$$r_o = 1.304 \text{ km}$$



central interval	$\Delta \eta'' = + .176''$
north interval	$\Delta \eta'' = + .663''$
south interval	$\Delta \eta'' = + .829''$
Average	$\Delta \eta'' = .461''$

For station #3 a single gradient central circle computation was carried out to obtain the effect of the 4.32km inner circle for the Complete Bouguer Anomaly Component. The Bouguer Correction Component was found to be zero. The results for the Complete Bouguer Anomaly Component are given below.

Complete Bouguer Anomaly Component

$$r_o = 4.32 \text{ km} \quad g_w = -120; \quad g_e = -127$$

$$\Delta \eta'' = .0525 [(-120) - (-127)] \quad -120 \quad -127$$

$$\Delta \eta'' = .357''$$

The correction component $\Delta \theta_p$ was found to be negligible at all of the stations.

To carry out the interpolation the quantity η_{gn} was computed at the three stations. Summarizing the results we have below:

Station 1

Bouguer Correction Component (4.32km to 55.66km)	-2.34"
Bouguer Correction Component (0 to 4.32km)	<u>-.42"</u>
TOTAL Bouguer Correction Component	-2.76"
Complete Bouguer Anomaly Component (4.32km to 55.66km)	+2.47"
Complete Bouguer Anomaly Component (0 to 4.32km)	<u>+.16"</u>
TOTAL Complete Bouguer Correction Component	+2.63"
$\Delta \theta_p$ Component	<u>0.00"</u>
TOTAL η_{gn} for Station 1	- .13"

Station 2

Bouguer Correction Component (4.32km to 55.66km)	-1.62"
Bouguer Correction Component (1.304km to 4.32km)	+ .82"
Bouguer Correction Component (0. to 1.304km)	+ .46"
TOTAL Bouguer Correction Component	- .34"
Complete Bouguer Anomaly Component (4.32km to 55.66km)	+1.87"
Complete Bouguer Anomaly Component (1.099km to 4.32km)	+ .05"
TOTAL Complete Bouguer Anomaly Component	+1.92"
$\Delta\theta_p$ Component	0.00"
TOTAL η_{g_n} for Station 2	+ 1.53"

Station 3

Bouguer Correction Component (4.32km to 55.66km)	-5.85"
Bouguer Correction Component (0 to 4.32km)	0.00"
TOTAL Bouguer Correction Component	-5.85
Complete Bouguer Anomaly Component (4.32km to 55.66km)	+3.11
Complete Bouguer Anomaly Component (0 to 4.32km)	+ .36
TOTAL Bouguer Correction Component	+3.47
$\Delta\theta_p$ Component	0.00
TOTAL η_{g_n} value for Station 3	-2.38

Because of the fact mentioned previously that the η_a values were picked from a contour map the values determined for the astro-geodetic deflections have considerable uncertainty. The values estimated for the astro-geodetic deflections were:

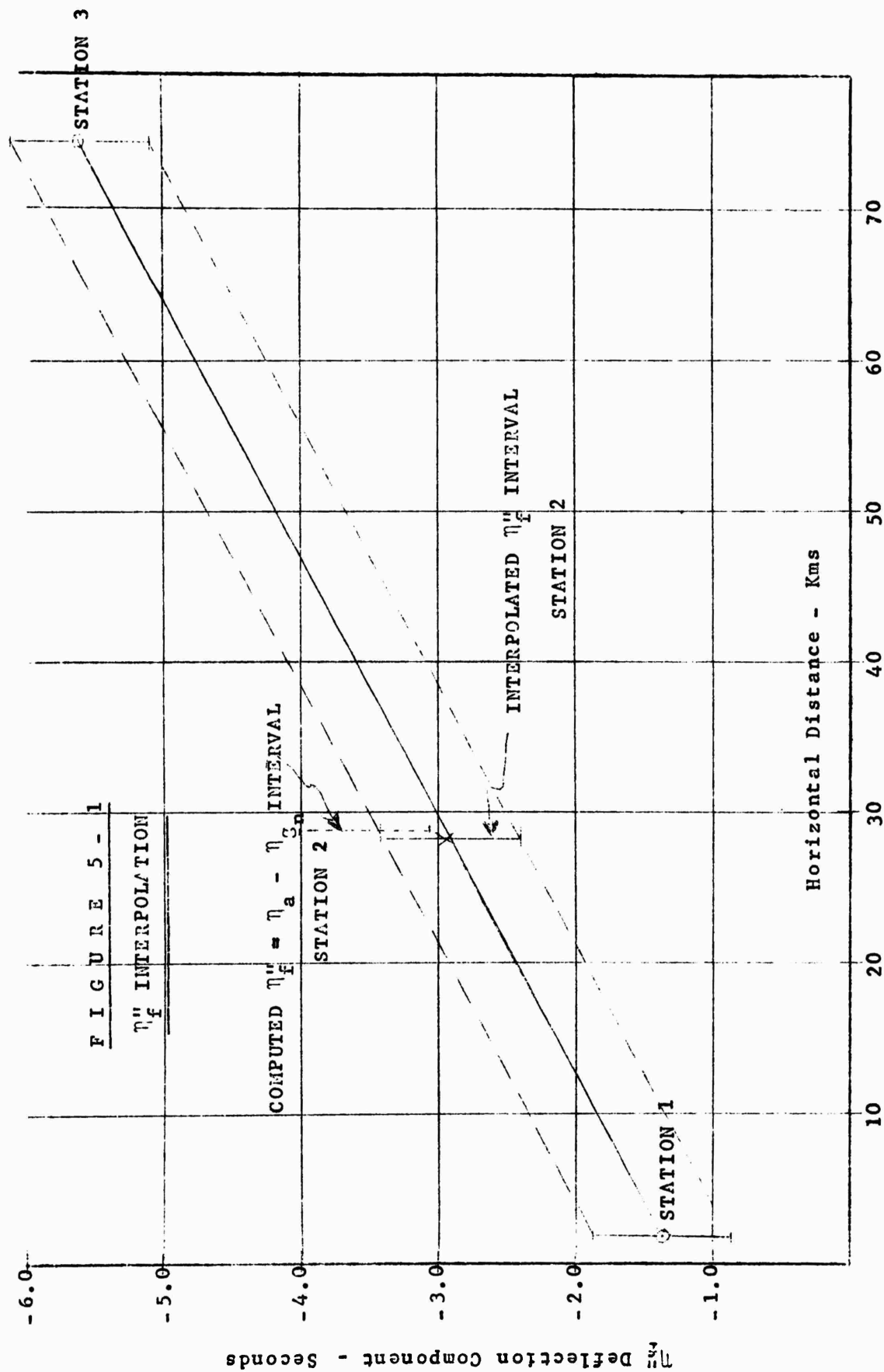
Station 1	$\eta_a = - 1.50'' \pm .5''$
Station 2	$\eta_a = - 2.00'' \pm .5''$
Station 3	$\eta_a = - 8.00'' \pm .5''$

Using the above η_a values and the η_{g_n} values computed previously the following values for η_f'' were determined at stations 1 and 3.

$$\text{Station 1} \quad \eta_f'' = \eta_a - \eta_{g_n} = - 1.37'' \pm .5$$

$$\text{Station 3} \quad \eta_f'' = \eta_a - \eta_{g_n} = - 5.62'' \pm .5$$

As shown in Figure 5-1 interpolation of the above values leads to an interpolated value at Station 2 of $\eta_f'' = - 2.91'' \pm .5$. If this is added to the value of η_{g_n} computed at Station 2 we obtain an interpolated value of $\eta = \eta_f'' + \eta_{g_n} = - 1.41 \pm .5$. The difference between the interpolated and the astro-geodetic deflection is therefore $\eta_a - \eta = - .59 \pm 1.0''$. The relation between the interpolated and the astro-geodetic deflection component is illustrated in a slightly different manner in Figure 5-1 where the computed value of η_f'' at Station 2 is compared with the interpolated value.



SECTION 6

SUMMARY AND CONCLUSIONS

In both the Test and Application Phases of this study, the results obtained with the proposed deflection interpolation method were excellent. In each case, the agreement between interpolated and observed deflection components was close enough that it was within the limits of sensitivity of the test data. The sensitivity of the Test Phase was controlled by the accuracy of the astro-geodetic deflection*components. The probable error claimed for the astro-geodetic deflections was $\pm .1''$ to $\pm .2''$. The results of the deflection computations of, for example, Rice (1952), however, show that the accuracy of astro-geodetic deflections is often much less. Since the astro-geodetic deflections used were the results of measurements made prior to 1920 a probable error of $\pm .2''$ would more than likely be optimistic. Under these conditions agreement of the interpolated and the astro-geodetic deflections to within $.22''$ can certainly be considered as within the limits of possible error in the astro-geodetic values.

As mentioned previously the accuracy of the astro-geodetic data used in the Application Phase was such that only errors in the interpolated deflections greater than $1.0''$ could be clearly determined. The astro-geodetic minus interpolated η deflection component difference of $.59'' \pm 1.0''$ is well within the limits of sensitivity of the data.

The accuracy of the results obtained with any gravimetric deflection interpolation procedure must be dependent upon the amount and quality of the gravity data available. In this respect the data available for both the Test and Application Phases leaves much to be desired. Indeed, the results would appear to be better than one should normally expect from the gravity coverage available. Unfortunately

extensive gravity data is not likely to be available in most rugged mountainous areas in the near future. Especially gravity data is not likely to be available in close spacing near astro-geodetic deflection stations unless special, expensive efforts are made to obtain it. It is, therefore, important to know if the apparent success obtained with the chosen deflection interpolation method using a minimum of gravity data is the result of a basic characteristic of the method or simply a result of luck.

The answer would seem to be a little of both. Although the writers would be the first to admit that the degree of accuracy obtained is unlikely to be always possible using comparable amounts of gravity data the deflection interpolation procedure chosen here does appear to allow optimum utilization of available data and to render unnecessary the carrying out of extremely close spaced surveys near deflection stations.

The reason satisfactory results can be obtained with the chosen method without an excess of gravity data can be seen from the nature of the equations and has been mentioned in the discussing of Part I of the final report. The gravitational effect of the topography is separated from the rest of the gravitational field and interpolated between gravity stations by using a topographic map. In few if any instances would it be possible to obtain sufficient gravity data to make direct interpolation of the gravitational effect of topography from the gravity maps more accurate than that obtained using elevation contour maps and an assumed density based on geologic knowledge. In the present problems the standard density of 2.67gm/cc has been used in the computations as being as good as any other. In areas such as the Gulf Coast where geologic knowledge indicates that the density of the majority of the topographic features is not 2.67gm/cc , the correct

density should be used.

With the topography accounted for one is interested only in obtaining sufficient data to accurately interpolate Complete Bouguer anomalies between observations. The Complete Bouguer anomaly is always a smoothly varying function and thus requires considerably fewer stations for its definition. By using geologic and geophysical information much of the variability in the Complete Bouguer anomaly can be understood and therefore better estimates of the variation between observation points made. Although how many or how few observation points are needed will ultimately depend upon the local situation, it is hard to imagine that there are many cases when a 10km grid of stations with perhaps 5 additional stations within 10km of the deflection station would not prove completely adequate. Of course, one is unlikely to often have gravity on a 10km grid but the above estimation is meant simply to show the order of station density at which one should aim. The point is that the addition of station density around a deflection station so that there are more than say 20 stations at a maximum within 10km of a deflection station is unlikely to lead to a very significant increase in the accuracy with which the gravity field can be derived. Attempts to obtain gravity stations at 1km spacing appear to be completely superfluous.

The results obtained were very encouraging and indicate the method used is a good one. To establish the method's actual degree of reliability, a more extensive test should be run involving the use of sets of three stations not in a line to interpolate both deflection components to a fourth station lying within the triangle of which the three stations are vertices. Eventually this type of interpolation might be used not only to establish intermediate deflection stations but to test the accuracy of astro-geodetic deflection stations and thus improve the astro-geodetic

deflection network by discovery and rejection of incorrect values.

As the primary purpose of the solutions obtained under the present contract was to test the accuracy of the deflection interpolation procedure using Bouguer anomalies, it is essential that a standard computational method such as the Rice template summation be used in obtaining the deflection component results.

Recommendations on Procedure

During the course of this work serious consideration was given to developing a computer technique for carrying out the computations along lines of the method utilized by Nagy (1962). However, a rather large programming job with a considerable amount of trial and error in order to arrive at an optimum procedure is involved. In addition elevation and Bouguer anomaly data would need to be averaged on an entirely different basis.

As useful results could not be obtained during the contract duration and as this was not an integral part of the contract the attempt was reluctantly abandoned. It is believed, however, that except for the area within about 15 km of the deflection station such a computer technique will ultimately be required for large scale problems. The computer method will become particularly important in the near future when very accurate 5' x 5' average elevations become available for large areas such as the continental United States.

BIBLIOGRAPHY

Heiskanen, W. A. and F. A. Vening Meinesz, 1958, "The Earth and its Gravity Field", McGraw-Hill Book Company, Inc., New York.
470 pp.

Molodenski, M. S., V. F. Eremeev, and M. I. Yurkina, 1960, "Methods for Study of the External Gravitational Field and Figure of the Earth", Central Research Institute of Geodesy, Aerial Photography and Cartography, Moscow, No. 131, (Trans by Israel Program for Scientific Translations, 1962) 248 pp.

Nagy, D., 1962, "Gravimetric Deflections of the Vertical by Digital Computer", Publication Dominion Observatory, Vol. 27, No. 1.

Rice, D. A., 1952, "Deflections of the vertical from gravity anomalies, Bulletin Geodesique, No. 25.

Strange, W. E. and G. P. Woollard, 1964, Anomaly Selection for Deflection Interpolation, Part 1: Theoretical Investigation, Hawaii Institute of Geophysics, Report 64-12.

USC and GS, Special Publication No. 229, 1941, Deflections of the Vertical in the United States.

A P P E N D I X

EXPLANATION OF TABLES

Final results can be obtained for Bouguer Correction Component and Complete Bouguer Anomaly Component from the tables in this Appendix as follows.

Test Phase

$$\begin{aligned}\text{Bouguer Correction Component} &= - (.03406)(.001) \text{ SUM X COS} \\ \text{Complete Bouguer Anomaly Component} &= + (.001) \text{ SUM X COS}\end{aligned}$$

Application Phase

$$\begin{aligned}\text{Bouguer Correction Component} &= - (.1117)(.001) \text{ SUM X SIN} \\ \text{Complete Bouguer Anomaly Component} &= + (.001) \text{ SUM X SIN}\end{aligned}$$

The change in sign between the Bouguer Correction Component and the Complete Bouguer Anomaly Component results from the fact that in the Tables the Complete Bouguer Anomalies have been listed as positive numbers to avoid needless repetition of the minus sign throughout the tables although the Complete Bouguer Anomalies used are negative. This is taken into account with a sign change in the summation equations above.

Table 1
DEFLECTION STATION 102
DEFLECTION RESULTS RICE CIRCLES 22 - 37
COMPARTMENT NUMBERS 1 - 18

Circle Number	Bouguer Correction Component																	
	1	2	3	4	5	6	7	8	9	10	11	12	13	14	15	16	17	18
22	6150	6150	6200	6200	6250	6200	6175	6150	6050	6025	6000	6000	6000	6000	5900	5950	6000	6025
23	6175	6200	6200	6300	6350	6300	6200	6175	6100	6000	6000	6000	6000	5900	5800	5900	6000	6000
24	6300	6350	6300	6600	6600	6300	6300	6200	6100	6075	6000	5950	5900	5900	5800	5900	5900	6000
25	6300	6600	6400	6400	6500	6400	6400	6300	6175	6100	6050	6000	5925	5850	5750	5850	5900	6000
26	6240	6450	6490	6480	6510	6530	6375	6310	6240	6175	6095	6025	5960	5850	5720	5805	5890	6040
27	6365	6520	6515	6740	6645	6560	6470	6400	6305	6150	6110	6050	5965	5620	5705	5805	5850	6000
28	6450	6650	6710	6750	6720	6635	6525	6425	6225	6115	6030	6005	5920	5780	5705	5780	5830	6035
29	6562	6804	6933	6891	6821	6704	5937	6420	6258	6054	5945	5866	5820	5795	5625	5741	5775	6005
30	6694	6916	7188	6319	6972	6819	6700	6538	6263	6100	5941	5811	5722	5688	5608	5633	5753	5877
31	6922	7155	7277	7305	7155	6915	6733	6611	6463	6350	6100	5877	6377	5636	5527	5611	5633	5938
32	7377	7533	7555	7480	6397	6905	6683	6516	6369	6261	6097	5936	5755	5566	5438	5428	5577	5844
33	6555	7463	7488	7450	7138	6833	6583	5688	6233	6091	5938	5792	5661	5561	5358	5402	5555	5788
34	7253	7227	7338	7269	7125	6771	6539	6308	6112	5949	5800	6225	5500	5375	5410	5260	5380	5800
35	7022	7067	7078	7133	6978	6739	6578	6439	6100	5950	5778	5522	5372	5233	5211	5200	5356	5611
36	6753	6342	6136	6694	6547	6518	6577	6636	6342	6048	5901	5549	5226	5109	5109	5138	5021	5138
37	6459	6166	6342	6342	6283	6195	6459	6166	6080	5725	5637	5461	5226	4962	4874	4991	4844	4932
SUM	105577	107593	108159	108353	106799	105314	103324	101282	99415	97168	95422	93469	92337	89825	88560	89394	90264	93033
SXCOS	105176	103924	98016	88763	75518	60408	43627	28212	8669	-8473	-24693	-39500	-52965	-63515	-72548	-81018	-87186	-92679

Complete Bouguer Anomaly Component

22	227	227	226	226	226	226	225	225	224	223	222	221	220	220	220	219	219	219
23	228	228	228	227	227	227	226	225	224	223	222	221	220	219	218	218	218	218
24	228	228	228	228	228	227	226	225	224	223	221	220	219	218	218	217	217	217
25	229	229	229	228	228	227	226	225	224	222	221	220	219	218	217	216	216	216
26	230	230	229	229	228	227	226	225	223	222	221	219	218	218	217	216	216	216
27	231	231	230	229	228	227	226	224	222	221	220	219	217	215	214	214	214	215
28	232	231	230	229	228	226	225	224	222	221	219	217	214	213	213	213	214	214
29	232	231	230	228	227	225	224	222	221	220	217	215	213	212	212	212	213	214
30	232	230	229	227	225	224	222	221	221	219	216	214	213	212	212	212	212	213
31	232	229	228	226	224	221	219	219	218	215	213	213	212	211	211	211	211	212
32	231	229	227	225	222	219	217	217	216	214	212	212	210	209	209	209	210	210
33	229	228	226	223	219	216	215	214	215	214	212	210	207	206	206	206	207	208
34	229	227	224	221	217	214	212	213	213	212	210	207	204	201	200	199	202	203
35	229	224	222	218	214	213	212	210	210	210	208	204	200	198	196	197	198	199
36	226	220	214	208	208	208	209	208	207	207	205	201	196	193	192	193	195	197
37	217	210	199	193	193	201	203	203	202	202	199	193	190	188	188	191	193	196
SUM	3662	3632	3599	3565	3542	3528	3515	3500	3488	3473	3442	3406	3372	3354	3344	3345	3357	3367
SXCOS	3648	3508	3262	2920	2505	2024	1485	906	304	-303	-891	-1439	-1934	-2372	-2739	-3032	-3243	-3354

Table 1 (cont.)
DEFLECTION STATION 102
DEFLECTION RESULTS RICE CIRCLES 22 - 37
COMPARTMENT NUMBERS 19 - 36

Bouguer Correction Component

	19	20	21	22	23	24	25	26	27	28	29	30	31	32	33	34	35	36
22	6100	6150	6200	6200	6400	6500	6500	6500	6400	6300	6200	6200	6175	6300	6300	6400	6175	6133
23	6000	6200	6300	6300	6500	7000	7000	6900	6600	6600	6400	6200	6300	6300	6400	6400	6200	6150
24	6200	6300	6600	6800	7000	7200	6800	7000	7600	7000	6500	6200	6300	6400	6500	6400	6300	6200
25	6300	6800	9000	1600	7000	7200	8000	7600	7800	7000	6800	6800	6600	6600	6500	6400	6375	6300
26	6400	7400	8520	6840	7560	8000	8060	9320	8320	8200	7040	6950	7180	7220	6760	6540	6410	6355
27	6300	7920	9960	8160	8360	9420	9000	9240	9960	8920	7960	7200	7700	7800	7400	7580	7580	7420
28	6360	7140	8360	8800	9680	10540	9920	10780	9980	9200	8840	7680	8360	8600	8400	7180	7720	7440
29	6291	7233	8266	8733	9866	10600	11100	11116	10416	10150	9200	8666	8233	9803	8950	7550	6750	6495
30	6233	6966	8266	9600	9700	10000	10777	11275	11828	12455	10111	9188	7966	9216	9244	8311	6950	6580
31	6483	6877	7800	9433	9544	9522	9944	10888	11722	12411	11144	9466	8555	9244	9111	8855	7694	6700
32	6277	6386	7511	8977	9422	9444	9822	10200	10548	10477	10178	9466	8733	9022	9127	8766	7088	6927
33	6150	6225	6711	7155	8655	9466	9777	9855	9646	9213	9604	9198	8888	8403	9086	8855	7663	7247
34	5967	6089	6400	7100	8472	8822	8711	8922	8689	8958	9060	9078	8952	8467	8856	9211	7711	7300
35	5128	5639	5778	6444	6856	6889	7678	7967	8333	8622	8589	8933	8722	8289	7933	9178	7244	6900
36	5226	5197	5373	5432	6019	7105	8221	8632	8749	9014	8280	8368	8162	7780	7575	7457	6489	6635
37	5138	5374	5578	6753	6929	6400	7780	6180	6102	9336	8984	9014	8544	7428	7311	7046	6048	6806
SUM	97053	103895	114623	123327	127963	134608	139090	145355	145953	143856	134890	128607	125370	126152	125453	122129	110397	107388
SXCOS	-96584	-100252	-103883	-98572	-90483	-77211	-58779	-37618	-12727	12544	34910	54349	71912	89202	10277	110686	106632	106980

Complete Bouguer Anomaly Component

	19	20	21	22	23	24	25	26	27	28	29	30	31	32	33	34	35	36
22	219	219	219	220	220	221	221	222	222	223	224	224	225	225	226	226	226	227
23	218	218	218	219	220	220	221	222	222	223	224	224	225	225	226	226	227	228
24	218	218	218	219	220	220	221	222	222	223	224	224	225	225	226	226	227	228
25	217	217	217	218	219	219	220	221	222	223	224	224	225	225	226	227	228	229
26	216	216	217	217	218	218	220	221	222	223	223	224	225	225	226	227	228	230
27	215	216	216	216	217	218	219	220	221	222	223	223	224	224	226	227	229	231
28	215	215	215	216	216	217	218	219	221	221	222	222	223	223	225	227	228	232
29	215	215	215	215	216	216	217	218	220	221	221	221	222	222	223	226	229	232
30	214	215	215	215	215	216	216	217	218	219	219	220	220	221	221	224	229	232
31	214	215	215	215	215	215	215	216	216	217	217	217	218	219	219	224	228	232
32	213	215	215	215	214	214	214	214	215	215	215	215	216	217	219	224	227	230
33	211	214	215	214	214	213	214	213	215	215	215	214	214	215	217	222	227	229
34	207	2142	215	213	213	214	214	215	216	216	220	218	216	214	215	220	227	231
35	202	210	215	216	217	217	217	219	220	220	220	218	216	214	215	217	226	231
36	202	209	215	220	222	222	222	222	227	228	228	226	222	219	214	215	226	231
37	200	208	216	229	230	227	228	232	238	239	238	235	229	222	215	214	221	221
SUM	3396	3434	3456	3476	3484	3485	3498	3516	3537	3548	3552	3546	3543	3543	3552	3586	3638	3672
SXCOS	-3383	-3317	-3132	-2848	-2464	-1990	-1478	-910	-308	309	919	1499	2032	2505	2910	3250	3638	3658

Table 2
DEFLECTION STATION 105
DEFLECTION RESULTS RICE CIRCLES 22 - 37
COMPARTMENT NUMBERS 1 - 18

Bouguer Correction Component																	
1	2	3	4	5	6	7	8	9	10	11	12	13	14	15	16	17	18
22	6700	6675	6600	6575	6550	6500	6475	6245	6400	6400	6375	6350	6350	6350	6350	6350	6375
23	6725	6700	6650	6600	6550	6445	6450	6425	6400	6400	6375	6375	6350	6350	6350	6350	6375
24	6700	6800	6600	6575	6550	6475	6425	6375	6350	6300	6325	6325	6300	6300	6275	6300	6350
25	6725	6700	6700	6650	6575	6475	6450	6425	6400	6300	6250	6250	6250	6250	6250	6250	6300
26	6800	6800	6750	6650	6600	6550	6500	6500	6450	6350	6258	6200	6200	6200	6200	6225	6250
27	7000	6900	6800	6775	6650	6600	6800	6750	6550	6425	6300	6200	6125	6125	6125	6150	6200
28	7200	6775	6700	6575	6550	6800	7000	6950	6625	6450	6350	6200	6100	6050	6075	6100	6150
29	6800	6800	6575	6575	6575	6700	6800	6850	6725	6475	6325	6250	6075	6000	6000	6030	6075
30	6400	6850	6700	6450	6375	6450	6600	6800	6675	6500	6300	6225	6150	5950	5900	5950	6000
31	6615	6564	6589	6625	6544	6574	6679	6600	6600	6600	6375	6200	6200	5975	5850	5825	5870
32	6737	6275	6270	6397	6132	6282	6608	6535	6430	6448	6422	6308	6147	6072	5915	5698	5693
33	6688	6478	6553	6226	6307	6168	6449	6328	6227	6272	6214	6164	6101	6050	5828	5579	5586
34	6701	6174	6207	6137	6281	6277	6367	6293	6148	5998	6002	5937	5847	5924	5662	5467	5457
35	6534	6056	6077	6107	6113	5962	6160	6131	5992	5829	5753	5712	5671	5718	5526	5317	5293
36	6136	5872	5960	5872	5843	5784	5901	5784	5666	5549	5432	5344	5373	5402	5373	5197	5109
37	5872	5843	5755	5696	5696	5637	5697	5608	5490	5402	5226	5167	5138	5167	5138	4962	4903
SUM	106333	104263	103536	102510	102091	101559	103211	103079	101873	100673	99257	97953	96823	96402	94817	93770	93986
SACOS	105929	100707	39835	83976	72189	58254	43617	26677	3883	-8779	-25688	-41395	-55538	-68166	-85933	-90572	-93629

Complete Bouguer Anomaly Component.

Complete Bouguer Anomaly Component.																	
1	2	3	4	5	6	7	8	9	10	11	12	13	14	15	16	17	18
22	214	214	214	214	214	214	213	213	213	213	213	213	213	213	213	213	214
23	214	213	213	213	213	213	213	213	213	213	213	213	213	213	213	214	214
24	213	213	213	213	213	213	212	212	212	212	212	212	212	213	213	213	214
25	213	213	212	212	212	212	212	212	212	212	212	212	212	212	213	213	214
26	213	213	212	212	212	212	212	211	211	211	211	211	211	212	212	213	214
27	214	213	212	211	211	211	211	210	210	210	209	210	211	211	212	213	214
28	214	213	212	211	210	210	210	210	209	208	208	209	210	211	212	213	214
29	213	212	211	209	209	209	209	209	208	207	208	209	210	211	212	213	214
30	212	210	209	207	208	208	208	208	207	207	207	208	209	210	212	213	214
31	209	206	205	204	204	205	207	207	206	206	207	208	209	210	212	212	213
32	204	202	200	201	201	202	203	203	203	204	205	207	208	208	208	208	208
33	198	196	195	195	197	199	200	201	201	200	201	202	204	206	206	205	205
34	192	191	191	190	191	194	196	198	197	197	198	199	201	202	203	201	201
35	189	186	185	175	186	186	188	189	190	191	192	194	195	195	196	196	197
36	184	179	178	179	180	181	181	182	182	184	186	187	188	188	190	191	193
37	177	172	172	172	174	175	175	176	177	180	181	180	181	182	185	186	189
SUM	3273	3246	3234	3228	3234	3244	3252	3258	3255	3256	3261	3267	3283	3292	3310	3314	3329
SACOS	3261	3135	2931	2644	2287	1861	1374	843	284	-284	-844	-1381	-1883	-2328	-3000	-3201	-3316

Table 2 (cont.)
 DEFLECTION STATION 105
 DEFLECTION RESULTS RICE CIRCLES 22 - 37
 COMPARTMENT NUMBERS 19 - 36

Bouguer Correction Component

Circle Number	19	20	21	22	23	24	25	26	27	28	29	30	31	32	33	34	35	36
22	6400	6450	6500	6550	6575	6600	6600	6625	6650	6700	6700	6725	6750	6725	6725	6725	6700	6700
23	6425	6475	6500	6025	6550	6575	6625	6650	6700	6750	6775	6800	6800	6800	67752	6750	6750	6750
24	6375	6425	6450	6525	6550	6575	6625	6650	6675	6700	6700	6725	6780	6750	6700	6675	6700	6650
25	6350	6400	6475	6550	6575	6600	6700	6775	6800	6850	6900	6900	6950	6850	6850	6800	6800	6750
26	6350	6375	6425	6500	6550	6600	6650	6700	6850	6925	6950	7000	7000	6950	6900	6875	6850	6800
27	6250	6300	6375	6475	6550	6600	6700	6800	6900	7000	7100	7150	7200	7000	7000	7000	7000	6900
28	6200	6300	6375	6500	6650	6700	6800	6900	7100	7200	7400	7400	7425	7200	7150	7150	7100	7200
29	6150	6300	6400	6425	6400	6650	6650	6750	6925	7200	7400	7400	7425	7400	7250	7300	7300	7000
30	6100	6200	6175	6150	6100	6400	6575	6725	6800	7175	7450	7600	7550	7400	7325	7175	7200	6750
31	5980	6080	6140	6020	6050	6250	6500	6680	6865	6150	7225	7600	7570	7560	7290	7225	7075	7100
32	5818	5958	5953	5823	6142	6130	6363	6728	6787	6932	7125	7558	7608	6228	7300	7042	6992	7040
33	5662	5752	5689	5746	5879	5947	6114	6266	6427	6592	6909	7418	7354	7252	7099	7013	6857	6852
34	5461	5584	5567	5572	5762	5956	6061	6425	7172	7102	6880	7176	7313	7093	6925	6891	6797	6672
35	5333	5408	5309	5637	6009	7542	8222	7778	8509	9000	8308	7440	7667	7022	6769	6772	6653	6548
36	5167	5226	5373	5755	6136	8514	10305	10687	9777	8984	8804	8602	7399	6665	6665	6371	6107	6136
37	5109	5109	5549	5931	6489	8368	9924	10305	9777	9131	8368	7957	7134	6136	6517	6166	5901	5931
SUM	95135	96322	97335	98184	100967	108007	113414	115344	110514	117086	116802	117301	115120	112431	111300	109930	108782	107779
SXCOS	-94773	-93037	-88215	-80432	-71394	-61953	-47929	-29851	-9637	10210	30228	49571	65975	79500	91177	99630	105073	107369

Complete Bouguer Anomaly Component

Circle Number	19	20	21	22	23	24	25	26	27	28	29	30	31	32	33	34	35	36
22	214	214	214	215	215	216	216	216	216	216	216	216	216	216	215	214	214	214
23	214	214	214	215	215	215	216	216	216	216	216	216	216	216	215	214	214	214
24	214	214	215	215	215	215	216	216	217	217	217	217	216	216	217	214	214	214
25	214	215	215	215	216	216	217	218	218	219	219	218	217	217	216	215	214	213
26	214	215	216	216	216	217	218	219	219	220	220	220	218	217	217	216	215	214
27	215	216	217	217	218	218	219	217	218	218	218	217	217	216	215	214	214	214
28	215	216	217	218	219	220	220	220	221	222	223	223	221	220	218	217	216	215
29	215	216	218	219	220	221	222	223	224	224	225	224	223	221	220	219	218	216
30	214	215	217	219	221	222	224	225	226	226	226	226	225	223	221	219	216	213
31	212	213	215	216	220	222	225	227	228	228	228	227	226	225	222	220	216	212
32	210	212	213	214	218	222	226	229	230	230	229	228	227	226	223	220	215	208
33	206	209	211	212	216	220	225	228	231	233	232	231	228	226	224	220	213	206
34	203	206	210	211	214	217	221	227	228	230	230	229	229	228	224	218	210	200
35	199	203	208	211	214	215	217	220	223	223	226	230	232	230	224	216	206	194
36	194	199	206	210	215	215	215	215	215	216	218	222	226	230	224	217	202	192
37	192	196	200	209	215	213	215	217	215	214	213	215	216	230	216	205	196	186
SUM	3345	3373	3406	3432	3467	3485	3512	3533	3545	3552	3556	3559	3553	3551	3509	3458	3393	3325
SXCOS	-3332	-3258	-3087	-2811	-2452	-1999	-1484	-914	-309	310	920	1504	2038	2511	2875	3134	3277	3312

Table 3

DEFLECTION STATION 116
DEFLECTION RESULTS RICE CIRCLES 22 - 37
COMPARTMENT NUMBERS 1 - 18

Bouguer Correction Component

	1	2	3	4	5	6	7	8	9	10	11	12	13	14	15	16	17	18
22	10300	9700	9500	9300	9200	9300	9500	9700	9600	9600	9700	10000	9300	9600	10000	9300	10200	11300
23	10200	9400	9010	9110	9000	9000	9000	9200	9425	9400	9500	9900	10335	10450	10775	11000	11350	11800
24	9800	9650	9000	8650	9200	8800	8700	9150	8800	9075	9425	10150	10200	11400	11500	10965	11400	11500
25	9400	9200	9000	8450	8500	8200	8900	8900	8395	10000	10200	10000	11300	11200	11800	11000	10975	11000
26	9341	8928	8300	7928	7566	7344	7403	7378	8753	8778	9803	10028	10065	10442	10603	11184	10778	10278
27	8453	8010	8360	8560	8780	8078	7305	6596	6910	7534	8120	8900	9260	10158	10800	10758	10120	9720
28	8240	8040	9390	9320	8740	8240	7360	6660	6580	6720	7520	7700	9100	9800	10060	9880	9810	9620
29	8530	9060	9440	8660	8770	9310	8630	8030	7592	7740	7920	8106	8260	9760	9854	9430	9430	9710
30	7633	7937	6933	7283	6258	5633	5417	5325	5233	5067	5045	6017	7517	6867	7358	8058	7882	9842
31	9192	8983	8975	6717	6841	6758	6492	6505	6508	6098	5950	6008	6900	7800	8000	8583	9425	9366
32	9072	8836	7608	6868	6679	6650	6656	6556	6330	6053	5861	5800	5968	6275	6800	7261	7822	7411
33	9063	8300	7114	7033	7073	7072	6954	6712	7407	6148	5929	5686	5706	5925	6284	6441	6644	6489
34	8919	7783	7308	7394	7531	7422	7169	6753	6411	6025	5781	5688	5556	5628	5950	5465	6175	6097
35	7889	6950	7067	7286	7594	7517	7169	6775	6517	6272	5936	5606	5398	5474	5650	5850	5722	5500
36	6694	6577	6782	6636	6400	6377	6753	6518	6224	5960	5784	5490	5373	5197	5432	5461	5373	5314
37	6547	6606	6606	6224	6518	6782	6636	6606	6224	5989	5896	5344	5167	5167	5079	5079	5109	5373
SUM	139273	134960	130399	125419	124450	122883	120044	117364	115009	116459	118170	120403	125405	131163	136151	135715	138213	140320
3xCOS	138744	130357	118180	102743	87999	70486	50731	30374	10028	-10155	-30582	-50882	-71932	-92745	-111534	-122452	-133500	-139787

Complete Bouguer Anomaly Component

	1	2	3	4	5	6	7	8	9	10	11	12	13	14	15	16	17	18
22	219	219	220	220	220	221	221	221	221	221	221	220	220	219	219	218	218	217
23	219	219	220	220	221	221	221	221	221	221	221	220	220	220	219	218	218	217
24	218	219	220	221	221	222	222	222	222	222	222	220	220	220	219	218	217	217
25	218	219	220	221	222	222	222	222	222	222	222	220	220	220	218	217	217	216
26	218	219	220	221	222	223	223	223	223	222	221	220	219	218	217	217	216	216
27	218	219	220	222	223	224	224	224	223	222	221	220	218	217	217	216	216	215
28	217	219	221	222	225	225	226	225	224	222	221	219	218	216	216	215	215	215
29	217	219	222	224	227	227	227	226	224	222	220	218	217	216	216	215	215	215
30	217	220	224	226	228	230	229	227	225	222	220	217	216	216	215	215	215	215
31	217	221	225	228	230	232	230	228	226	222	219	216	215	215	215	215	215	215
32	217	223	226	230	232	232	231	229	226	222	218	215	214	215	215	215	215	215
33	219	225	228	231	231	229	228	226	224	220	216	213	212	212	213	214	215	215
34	220	224	231	229	229	228	225	223	221	218	213	211	211	210	210	212	215	215
35	222	230	230	228	227	225	221	219	218	216	213	209	208	207	205	205	210	214
36	222	230	220	225	223	220	216	215	214	214	209	205	201	199	199	200	203	210
37	220	223	220	217	214	212	213	212	210	211	206	200	195	194	195	196	199	207
SUM	3498	3553	3577	3585	3595	3593	3579	3562	3544	3518	3481	3443	3424	3410	3407	3407	3419	3434
3xCOS	3485	3432	3242	2937	2542	2061	1512	922	309	-307	-901	-1455	-1964	-2411	-2791	-3088	-3302	-3421

Table 3 (cont.)
DEFLECTION STATION 116
DEFLECTION RESULTS RICE CIRCLES 22 - 37
COMPARTMENT NUMBERS 19 - 36

Circle Number	Bouguer Correction Component																		Circle Number
	19	20	21	22	23	24	25	26	27	28	29	30	31	32	33	34	35	36	
22	12100	12000	11400	11900	11500	11500	12000	12000	12100	11900	11800	11600	11600	12100	12300	12400	11600	9800	22
23	12075	11550	10780	11150	10800	11200	11000	11400	11000	10975	10700	10750	11100	11300	10800	10750	10800	10625	23
24	11200	10500	10600	10900	10500	10300	10900	10900	10200	10325	10200	10400	10750	10600	10000	9800	9950	9600	24
25	10220	10375	10545	10350	10295	10000	9900	9900	9700	9900	10600	10375	10300	9800	9600	9600	9600	9510	25
26	10078	10425	10494	10150	10000	9963	9938	9775	9363	9350	9675	9900	9856	9975	9650	9570	9469	9338	26
27	10020	9700	9620	9850	9800	10000	9650	9440	8940	7760	7560	7380	7180	7640	7660	7240	7210	7260	27
28	9710	9670	9830	9520	9680	9720	9280	9280	9210	7930	7670	7380	7180	7436	7220	7270	7070	6890	28
29	9342	9730	9740	10000	9590	9540	8620	8900	8820	8940	8790	9250	9160	7542	7725	7483	7208	7667	29
30	7758	8000	8383	8362	8350	8542	8108	8067	7358	7142	7383	7433	7487	7568	9160	9090	9112	8490	30
31	9216	10100	9300	9585	8407	7750	6033	8133	8550	8733	8642	8533	8768	8975	8636	8921	8550	8425	31
32	8200	8600	022	7211	7556	7722	8183	8282	8522	8789	8689	8331	8672	8978	8878	8372	8311	8383	32
33	7311	8422	822	6950	8211	8078	8533	8537	8828	9119	8567	8411	8500	9000	8700	8417	8223	9067	33
34	6119	7630	150	7019	7952	8375	9064	9276	9286	9100	8864	8517	8286	8144	8500	8200	8183	8461	34
35	5628	5644	5911	7100	7311	7878	8556	8844	9778	9189	8731	9400	8644	9156	7644	7644	7267	8422	35
36	5373	5608	6489	6312	7164	8573	8925	9313	9513	9014	8749	9248	9689	9102	8808	7780	7281	7134	36
37	5755	6723	7604	7457	7311	9219	9806	9953	9689	9307	8925	9248	9307	10217	9425	7839	6782	6723	37
SUM	140105	144077	141690	144164	144427	148360	148976	152290	150757	147473	145545	146316	146799	147533	144706	140576	136615	135795	
SXCOS	-139573	-139683	-128414	-118099	-102124	-85099	-62957	-39413	-9222	12860	37667	61833	84204	104321	118543	127404	131956	135279	

Complete Bouguer Anomaly Component

Circle Number	Complete Bouguer Anomaly Component																		Circle Number
	22	23	24	25	26	27	28	29	30	31	32	33	34	35	36	37	38	39	
22	217	216	216	215	215	215	215	215	215	215	215	215	216	216	216	216	218	218	22
23	217	216	216	215	215	215	215	215	215	215	215	215	216	216	216	216	218	218	23
24	216	216	215	215	215	215	215	215	215	215	215	215	216	216	216	216	218	218	24
25	216	216	215	215	215	215	215	215	215	215	215	215	216	216	216	216	218	218	25
26	216	215	215	215	215	215	215	215	215	215	215	215	216	216	216	216	218	218	26
27	215	215	215	215	215	215	215	215	215	215	215	215	216	216	216	216	218	218	27
28	215	215	214	215	215	215	215	215	215	215	215	215	216	216	216	216	218	218	28
29	215	215	214	213	213	213	214	215	216	216	215	215	215	215	215	214	215	216	29
30	215	214	214	213	214	215	215	215	216	216	216	216	216	215	215	214	215	216	30
31	214	213	213	214	215	216	217	217	219	219	219	218	217	216	215	214	214	215	31
32	213	214	215	216	217	218	219	220	222	223	224	223	220	217	215	214	214	215	32
33	213	215	217	217	219	222	225	224	226	228	228	227	225	221	217	215	213	215	33
34	214	217	219	220	222	225	228	228	233	234	235	233	229	225	220	216	213	215	34
35	216	221	224	224	226	229	229	229	237	244	245	244	234	230	224	217	214	215	35
36	219	228	229	229	229	235	235	235	250	255	260	255	241	235	228	223	215	214	36
37	213	218	226	230	232	240	250	260	262	263	263	261	255	248	238	231	223	211	37
SUM	3464	3464	3478	3481	3489	3522	3548	3579	3602	3602	3611	3582	3550	3518	3485	3460	3490	3452	
SXCOS	-3431	-3358	-3152	-2852	-2467	-2020	-1499	-926	-314	315	932	1514	2036	2488	2855	3136	3319	3439	

Table 4

DEFLECTION STATION 102

BOUGUER CORRECTION COMPONENT

RICE KINGS 14-21

	14	15	16	17	18	19	20	21	SUM	SUM X COS
1	6025	6030	6060	6060	6060	6100	6110	6130	48575	48390
2	6012	6025	6040	6050	6060	6100	6110	6130	48527	46872
3	6025	6050	6050	6075	6090	6100	6100	6180	48670	44109
4	6033	6060	6075	6100	6060	6150	6160	6210	48848	40016
5	6050	6060	6080	6100	6150	6200	6190	6200	49030	34669
6	6050	6060	6080	6100	6150	6200	6200	6200	49040	28129
7	6050	6060	6080	6100	6110	6150	6180	6190	48920	20673
8	6033	6040	6050	6060	6075	6100	6130	6150	48638	12587
9	6025	6040	6050	6060	6080	6100	6110	6110	48575	4235
10	6050	6050	6080	6100	6100	6090	6060	6060	48590	-4237
11	6040	6050	6075	6100	6090	6050	6000	6000	48405	-12527
12	6040	6050	6075	6075	6050	6000	5980	5950	48220	-20377
13	6030	6060	6060	6050	6010	5980	5900	5980	48070	-27572
14	6025	6030	6040	6025	6010	5950	5910	6000	47990	-33933
15	6015	6025	6000	6000	5980	5930	5900	5890	47740	-39108
16	6005	6010	6000	6000	5900	5880	5880	5880	47555	-43099
17	5990	6000	6000	5900	5890	5900	5900	5900	47480	-45860
18	5960	5950	5930	5900	5900	5940	5950	5980	47510	-47329
19	5950	5920	5900	5900	5930	5950	5990	6000	47540	-47359
20	5940	5920	5970	5900	5950	5930	6000	6080	47630	-46005
21	5950	5930	5910	5930	5980	6000	6000	6050	47750	-43275
22	5950	5930	5930	5950	5990	6030	6040	6080	47960	-39239

Table 4 (cont.)

DEFLECTION STATION 102
BOUGUER CORRECTION COMPONENT
RICE RINGS 14-21

	14	15	16	17	18	19	20	21	SUM	SUM X COS
23	5950	5950	5940	5980	6000	6130	6090	6190	48230	-34103
24	5960	5950	5950	5990	6050	6050	6150	6230	48330	-27724
25	5960	5960	5960	5990	6050	6080	6090	6190	48280	-20403
26	5980	5980	5980	5990	6050	6130	6180	6190	48480	-12546
27	5980	5980	5990	5990	6000	6100	6180	6230	48450	-4224
28	5980	5990	6000	6050	6010	6030	6080	6100	48240	4206
29	5980	6000	6100	6100	6090	6090	6050	6060	48470	12544
30	5990	6000	6100	6100	6100	6190	6100	6160	48740	20597
31	6000	6000	6100	6100	6150	6150	6160	6230	48890	28043
32	6000	6000	6080	6080	6150	6200	6220	6260	48990	34640
33	6010	6000	6030	6000	6090	6190	6140	6160	48620	39829
34	6010	6010	6010	6020	6030	6050	6090	6140	48360	43828
35	6020	6020	6030	6030	6050	6075	6090	6090	48405	46754
36	6030	6030	6050	6050	6060	6080	6100	6110	48510	48325

Table 5

DEFLECTION STATION 116
BOUGUER CORRECTION COMPONENT
RICE ~~KINGS~~ 14-21

	14	15	16	17	18	19	20	21	SUM	SUM X COS
1	11900	11450	11700	11900	11500	10833	10825	10425	90533	90189
2	11900	11500	11200	11200	11667	10933	10425	10025	88850	85820
3	12000	11600	11250	11250	11167	10767	10300	8788	87122	78958
4	12200	11700	11400	11100	10917	10750	10500	9650	88217	72267
5	12500	12200	11700	11150	10767	10583	10550	9650	89100	63002
6	12800	12400	11900	11350	10800	10367	10325	10175	90117	51691
7	12700	12550	12200	11450	11067	10433	10100	9975	90475	38234
8	12450	12300	12000	11600	11067	10500	10162	9912	89991	23289
9	12300	12000	11700	11400	11000	10533	10200	9825	88958	7757
10	12400	12050	11900	11600	11167	10767	10300	9838	90022	-7850
11	12500	12150	12000	11600	11450	11000	10362	10000	91062	-23567
12	12100	11900	11350	11538	11467	11033	10600	10175	90163	-38103
13	12050	12300	11800	11800	11767	10933	11250	10825	92725	-53187
14	12600	12800	12400	12350	12300	12167	11900	11175	97692	-69078
15	13300	13100	12900	12600	12400	12317	12012	11425	100054	-81964
16	13300	12850	12650	12400	12250	11933	11788	11575	98746	-89493
17	13150	12800	12600	12200	11900	11816	11575	11375	97416	-94094
18	13100	12850	12600	12300	12267	11667	11362	11400	97546	-97175
19	13050	12700	12450	12350	12100	11733	11725	11900	98008	-97635
20	13150	12800	12500	12250	12083	11917	11859	11975	98534	-95174
21	13150	12800	12500	12350	12300	11967	11744	11900	98711	-89462
22	13000	12700	12350	12325	12133	11900	11744	11662	97814	-80129

Table 5 (cont.)

DEFLECTION STATION 116

BOUGUER CORRECTION COMPONENT

RICE RINGS 14-21

	14	15	16	17	18	19	20	21	SUM	SUM X COS
23	12800	12600	12350	12150	12083	11883	11685	11950	97501	-68943
24	12700	12250	12175	12088	12050	11900	11794	11900	96857	-55557
25	12500	12300	12300	12175	12100	11888	11850	11625	96738	-40881
26	12450	12500	12500	12400	12300	11834	11912	11925	97821	-25316
27	12550	13000	12800	12725	12367	12000	11875	12175	99492	- 8675
28	12450	13000	12900	12775	12780	12200	12100	12450	100655	8777
29	13000	13000	12900	12600	12500	12092	12225	12512	100829	26094
30	13050	13050	13000	12600	12267	12100	12325	12625	101017	42690
31	13200	13100	13360	12900	12600	12467	12375	12675	102677	58895
32	13145	13100	13000	13150	12900	12833	12375	12638	103141	72931
33	13000	13000	12700	12250	12267	12500	12738	12100	100555	82374
34	12400	12500	12500	11750	11367	11767	11975	11825	96084	87081
35	11850	11300	12300	11750	11333	11233	11250	11025	92041	88902
36	11900	11600	11550	13900	11633	10950	11228	10912	93673	93317

TABLE 6

STATION 116

$\Delta\theta_p$ CORRECTION - RINGS A, B, AND C

	RING A		RING B		RING C		$\Delta\theta_p$ DEFL. CMPNT: 2 $\times 10^{-2}$
	AVG. CMPRT. HEIGHT	AVG. HEIGHT DIFF.	AVG. CMPRT. HEIGHT	AVG. HEIGHT DIFF.	AVG. CMPRT. HEIGHT	AVG. HEIGHT DIFF.	
1	13250	.80	12700	1.35	12370	1.68	9.66
2	13250	.80	12900	1.15	12430	1.62	8.21
3	13300	.75	13100	.95	12500	1.55	6.06
4	13450	.60	13250	.80	12670	1.38	3.13
5	13650	.40	13400	.65	12930	1.12	1.09
6	13750	.30	13550	.50	13230	.82	.36
7	13850	.20	13500	.55	13000	1.05	.32
8	13800	.25	13400	.65	12800	1.25	.34
9	13750	.30	13150	.90	12800	1.25	.17
10	13700	.35	13200	.85	12800	1.25	.17
11	13750	.30	13300	.75	12970	1.08	.32
12	13800	.25	13400	.65	12570	1.48	.30
13	13800	.25	13400	.65	12430	1.62	1.33
14	13950	.10	13350	.70	12530	1.52	1.36
15	13950	.10	13400	.65	12830	1.22	.90
16	13950	.10	13550	.50	13470	.53	.20
17	13900	.15	13430	.62	13500	.55	.34
18	13850	.20	13680	.37	13380	.67	.26
19	13750	.30	13600	.45	13300	.75	.54
20	13750	.30	13550	.50	13300	.75	.55
21	13750	.30	13400	.65	13380	.67	.62
22	13800	.25	13450	.60	13200	.85	.54
23	13800	.25	13400	.65	13100	.95	.53

TABLE 6 (cont.)

STATION 116

$\Delta\theta_p$ CORRECTION - RINGS A, B, AND C.

	RING A		RING B		RING C		$\Delta\theta_p$ DEFL. CMPNT: $\times 10^{-2}$
	AVG. CMPRT. HEIGHT	AVG. HEIGHT DIFF.	AVG. CMPRT. HEIGHT	AVG. HEIGHT DIFF.	AVG. CMPRT. HEIGHT	AVG. HEIGHT DIFF.	
24	13800	.25	13430	.62	13030	1.02	- .50
25	13800	.25	13430	.62	13000	1.05	- .39
26	13780	.27	13430	.62	13000	1.05	- .25
27	13750	.30	13400	.65	13000	1.05	- .09
28	13500	.55	13380	.67	13100	.95	.09
29	13750	.30	13450	.60	13200	.85	.19
30	13750	.30	13480	.57	13280	.77	.27
31	13750	.30	13480	.57	13310	.74	.36
32	13800	.25	13480	.57	13350	.70	.36
33	13700	.35	13450	.60	13100	.95	.84
34	13600	.45	13100	.95	12870	1.18	2.27
35	13400	.65	12800	1.25	12180	1.87	7.34
36	13250	.80	12650	1.40	12130	1.37	10.64

TABLE 7

STATION 116

$\Delta\theta_p$ CORRECTION - RINGS D, E, AND F

	RING D		RING E		RING F		
	AVG. CMPRT. HEIGHT	AVG. HEIGHT DIFF.	AVG. CMPRT. HEIGHT	AVG. HEIGHT DIFF.	AVG. CMPRT. HEIGHT	AVG. CMPRT. DIFF.	$\Delta\theta_p$ DEFL. CMPNT
1	11600	2.45	11400	2.65	10400	3.65	.109
2	11400	2.65	10900	3.15	10100	3.95	.137
3	11800	2.25	10800	3.25	10200	3.85	.088
4	12000	2.05	10600	3.45	10100	3.95	.066
5	12200	1.85	10600	3.45	10000	4.05	.036
6	12000	2.05	10800	3.45	10000	4.05	.014
7	12000	2.05	11000	3.05	10200	3.85	-.012
8	12000	2.05	11300	2.75	10300	3.75	-.034
9	12000	2.05	11500	2.55	11200	2.85	-.044
10	12600	1.45	12400	1.65	11800	2.25	-.019
11	12800	1.25	12200	1.85	11700	2.35	-.019
12	12800	1.25	11900	2.15	11400	2.65	-.026
13	12800	1.25	12000	2.05	11800	2.25	-.022
14	12900	1.15	12200	1.85	11800	2.25	-.017
15	12700	1.35	12100	1.95	11700	2.35	-.019
16	12500	1.55	12100	1.95	11700	2.35	-.018
17	12500	1.55	12100	1.95	11800	2.25	-.012
18	12700	1.35	12400	1.65	11900	2.15	-.003
19	13000	1.05	12600	1.45	12200	1.85	.002
20	13100	.95	12300	1.75	12400	1.65	.005

-14-

TABLE 7 (cont.)

STATION 116

$\Delta\theta_p$ CORRECTION - RINGS D, E, AND F

	RING D		RING E		RING F		$\Delta\theta_p$ DEFL. CMPNT.
	AVG. CMPRT. HEIGHT	AVG. HEIGHT DIFF.	AVG. CMPRT. HEIGHT	AVG. HEIGHT DIFF.	AVG. CMPRT. HEIGHT	AVG. HEIGHT DIFF.	
21	13100	.95	12800	1.25	12600	1.45	.005
22	12800	1.25	12400	1.65	12500	1.55	.043
23	12200	1.85	11300	2.75	11500	2.55	.054
24	11900	2.15	11400	2.65	11000	3.05	.080

Table 8
DEFLECTION STATION # 1
BOUGUER CORRECTION COMPONENT
RICE RINGS 22-36 COMPARTMENT NOS. 1-18

	1	2	3	4	5	6	7	8	9	10	11	12	13	14	15	16	17	18
22	550	550	550	500	550	550	550	550	550	550	550	500	500	525	550	550	550	525
23	550	525	500	575	575	575	550	550	550	550	550	525	525	500	525	550	550	550
24	525	500	600	600	600	600	600	600	525	550	550	550	550	500	525	550	500	500
25	500	500	600	625	625	625	700	650	600	550	500	500	550	550	500	550	500	550
26	550	500	550	625	600	625	660	700	700	640	600	550	550	550	500	550	500	600
27	560	500	500	500	590	650	655	700	700	700	720	630	550	550	500	500	500	640
28	490	450	475	540	600	600	630	640	635	740	800	680	575	555	505	525	570	515
29	480	475	475	530	630	630	640	630	790	860	810	320	630	545	535	525	515	480
30	480	500	495	535	560	685	670	810	850	830	890	330	780	520	500	485	475	500
31	435	450	440	480	560	540	600	760	670	780	950	1160	630	510	430	505	675	740
32	425	439	461	403	483	500	547	647	728	734	350	1078	617	500	506	833	881	911
33	475	494	528	517	494	556	592	644	628	722	833	928	606	533	811	1033	958	1083
34	456	467	511	486	517	514	586	578	725	789	884	1011	822	756	1300	1222	1133	1322
35	528	525	472	433	506	542	528	553	675	922	872	861	1208	864	1067	1500	1473	1156
36	600	483	492	450	446	475	467	562	700	1067	1467	1600	1067	1567	1417	1917	1633	1616
SUM	7604	7358	7649	7849	8336	8667	8975	9574	10026	10979	11831	12223	10210	9525	10221	11845	11418	11688
SxSIN	663	1904	3232	4502	5894	7100	8134	9248	9938	10937	11428	11073	8364	6735	5863	5006	2955	1019

Table 8
DEFLECTION STATION # 1
BOUGUER CORRECTION COMPONENT
RICE RINGS 22-36 COMPARTMENT NOS. 19-36

	19	20	21	22	23	24	25	26	27	28	29	30	31	32	33	34	35	36
22	525	550	650	650	650	650	650	600	550	550	550	550	550	550	550	500	500	500
23	500	600	700	700	650	650	650	650	600	500	550	550	550	550	550	550	500	525
24	600	700	650	650	650	600	600	650	650	550	525	550	550	550	550	500	550	550
25	700	700	650	650	600	600	500	550	600	600	500	500	550	550	550	500	550	550
26	760	720	640	570	500	500	500	500	500	560	530	500	500	500	500	550	550	570
27	600	540	535	475	475	475	475	475	500	500	500	500	500	500	500	540	570	600
28	485	475	475	495	515	430	520	540	490	450	510	450	450	450	500	520	555	570
29	485	520	580	530	600	660	640	600	600	455	480	430	480	450	500	500	470	450
30	600	630	630	720	650	650	580	590	525	440	500	475	475	465	455	570	570	530
31	690	690	590	550	540	490	505	530	530	505	480	570	570	475	425	445	470	445
32	978	836	603	464	419	422	422	431	422	544	503	533	544	511	425	433	425	428
33	964	853	675	514	439	583	672	575	481	432	458	492	519	456	500	439	450	453
34	1056	828	578	578	517	556	592	550	523	461	394	433	422	444	422	489	536	489
35	828	828	756	522	525	628	731	644	522	450	500	517	406	450	528	522	628	533
36	1000	996	562	600	575	633	500	583	500	550	533	483	592	717	767	767	667	703
SUM	10771	10466	9279	8668	8305	8577	8477	8468	7993	7546	7518	7633	7658	7618	7722	7875	7991	7951
SxSIN	-939	-2709	-3921	-4972	-5872	-7026	-7633	-8179	-7963	-7517	-7262	-6918	-6273	-5387	-4429	-3323	-2068	-693

Table 9

DEFLECTION STATION # 2
BOUGUER CORRECTION COMPONENT
RICE RINGS 22-36 COMPARTMENT NOS. 1-13

	1	2	3	4	5	6	7	8	9	10	11	12	13	14	15	16	17	13
22	700	700	700	650	650	650	600	600	600	600	650	700	700	700	700	700	700	800
23	700	650	650	650	650	600	700	750	600	700	800	700	600	700	700	800	950	1000
24	700	700	700	750	600	700	600	650	600	700	300	700	750	700	700	750	1000	1000
25	600	575	550	550	600	700	725	700	600	650	700	750	850	800	700	850	900	1000
26	550	550	550	550	630	620	710	790	780	800	790	780	860	970	730	760	920	1040
27	600	630	580	550	530	550	620	640	720	750	830	850	780	840	690	760	810	900
28	810	760	820	730	910	900	583	650	770	855	1000	340	900	940	830	750	900	850
29	555	654	654	636	544	533	610	596	710	870	955	890	860	1030	815	870	1134	850
30	516	526	520	540	534	525	620	660	760	870	990	1090	1080	1080	1200	970	900	565
31	483	485	480	485	490	540	710	740	640	850	960	1020	1260	1020	1000	1440	1120	485
32	499	527	563	491	489	500	617	650	339	861	1511	1472	1511	1411	1256	1367	1089	502
33	569	486	476	458	428	442	497	739	961	966	1056	1722	1317	1472	1475	622	1011	700
34	390	427	377	375	375	375	389	722	922	806	1200	733	961	1589	831	1433	1737	878
35	456	414	467	467	384	375	375	564	534	431	439	461	717	1589	1367	1733	1689	900
36	533	554	525	550	450	446	413	446	450	729	800	1483	1317	762	1650	1800	1583	1583
SUM	8661	8638	8612	8432	8264	8456	8769	9897	10486	11438	13531	14191	14463	15653	14644	15605	16523	13153
SxSIN	755	2236	3639	4837	5843	6927	7947	9560	10446	11395	13070	12891	11348	11068	8400	6595	4276	1147

Table 9
DEFLECTION STATION # 2
BOUGUER CORRECTION COMPONENT
RICE RINGS 22-36 COMPARTMENT NOS. 19-36

	19	20	21	22	23	24	25	26	27	28	29	30	31	32	33	34	35	36
22	900	950	1000	900	900	900	900	900	900	900	850	800	800	700	700	700	700	700
23	300	900	1000	1100	1050	900	900	900	900	800	800	700	700	700	700	700	750	700
24	850	1100	1150	1000	1000	850	800	850	900	900	800	300	800	850	700	300	750	700
25	1000	1150	1100	1000	900	800	800	700	900	800	800	800	700	700	600	550	650	600
26	1100	960	1030	1060	930	740	940	770	750	900	300	800	300	800	610	550	575	570
27	1040	340	1090	920	310	920	340	830	700	340	710	800	710	660	585	757	550	550
28	810	760	820	730	910	900	880	800	750	680	615	670	640	650	590	524	516	548
29	595	570	590	670	710	650	650	720	660	725	710	610	650	590	532	470	485	496
30	480	480	450	555	524	572	560	470	505	595	595	620	700	580	560	605	605	580
31	480	480	470	429	470	518	490	500	515	552	625	495	530	530	490	445	510	525
32	1067	911	703	505	388	517	547	485	424	403	527	493	489	482	400	459	434	502
33	1500	1031	1144	967	642	444	469	653	611	475	522	533	495	439	477	543	473	539
34	1673	1267	906	989	978	679	561	435	456	462	476	459	460	437	478	461	587	397
35	1635	1778	1267	1261	753	722	550	650	561	458	471	421	415	444	437	436	461	466
36	1567	1517	1333	842	946	571	416	483	479	491	608	475	500	525	583	542	483	508
SUM	15502	14644	14058	13028	11966	10683	10203	10151	10011	10076	9909	9481	9389	9087	8442	3410	8584	8331
SxSIN	-1352	-3790	-5941	-7473	-8461	-8671	-9247	-9805	-9973	-10038	-9571	-8593	-7691	-6425	-4842	-3550	-2222	-731

Table 10
DEFLECTION STATION # 3
BOUCUER CORRECTION COMPONENT
RICE RINGS 22-36 COMPARTMENT NOS. 1-13

	1	2	3	4	5	6	7	8	9	10	11	12	13	14	15	16	17	18
22	450	450	450	450	450	450	450	450	475	500	600	600	600	700	700	650	550	475
23	475	450	450	450	450	450	450	475	475	750	800	850	850	1100	1000	900	700	550
24	475	450	450	450	450	450	450	475	700	1000	1200	1200	1300	1300	1200	1000	800	600
25	475	475	450	450	450	450	475	475	800	1300	1200	1200	1300	1500	1300	800	700	550
26	450	450	450	450	450	450	540	480	810	1120	1150	980	1130	1330	1040	830	690	520
27	425	430	450	450	450	530	960	990	890	960	1150	1420	1420	1300	1040	1080	860	530
28	375	385	450	450	620	650	910	1230	1310	1340	1580	1420	1660	1420	1420	1220	830	630
29	375	375	400	700	640	830	920	800	1160	1300	1240	1320	1600	1540	1340	1180	1240	710
30	375	375	590	890	610	600	800	700	1300	1300	1180	1840	1600	1560	1460	1440	770	490
31	445	465	655	680	860	680	740	780	1120	1260	1440	1480	1740	1380	1230	730	590	840
32	494	533	603	772	750	778	906	594	1389	1283	1267	1656	1311	1611	1389	609	1378	1489
33	528	525	597	744	822	806	1144	1056	1122	1389	1311	1700	1556	1794	1078	1178	1333	1722
34	565	569	578	656	756	856	1167	1267	1330	1659	1711	1389	1866	1733	1344	1411	2044	2300
35	642	419	619	747	761	1005	1150	1244	1144	1777	1622	1766	2100	1722	1455	1677	1922	1355
36	590	667	679	704	833	867	862	962	1183	1483	1500	2233	2050	2167	1417	1850	1533	1433
SUM	7138	7218	7871	9043	9352	9852	11924	12278	15208	18421	18951	21554	22083	22077	18463	16605	15940	14194

SKIN 622 1868 3326 5187 6613 8071 10807 11859 15150 18351 18305 19534 18090 15610 10590 7017 4125 1238

Table 10
DEFLECTION STATION # 3
BOUGUER CORRECTION COMPONENT

RICE RINGS 22-36 COMPARTMENT NOS. 19-36

	19	20	21	22	23	24	25	26	27	28	29	30	31	32	33	34	35	36
22	450	475	475	450	450	450	450	450	450	450	450	475	500	600	500	475	450	450
23	475	475	450	450	450	450	450	450	450	475	475	650	700	600	500	500	475	450
24	500	475	450	450	450	450	450	450	475	475	600	900	800	750	750	750	650	500
25	500	475	450	450	475	450	450	450	500	600	800	1000	750	750	750	650	500	450
26	450	450	450	450	505	450	475	570	630	730	960	1030	850	780	770	540	410	450
27	425	450	450	425	690	690	650	330	1000	1090	1070	1010	910	710	500	410	400	450
28	530	450	450	450	940	770	960	1040	930	950	370	940	830	615	435	375	380	415
29	560	540	490	465	980	900	930	960	950	970	870	810	610	400	375	375	375	375
30	570	560	540	450	1100	1220	920	320	890	390	850	570	490	385	375	375	375	375
31	1280	1060	470	450	1140	1740	1140	960	330	750	660	590	465	400	375	375	375	400
32	1633	1233	475	558	1244	1933	1344	956	817	700	766	622	475	392	375	375	422	472
33	1656	839	783	1300	1283	1444	1200	1050	922	633	625	533	481	406	475	475	422	497
34	2167	944	1156	1367	1378	1389	1051	956	873	750	578	517	481	397	375	378	422	494
35	1255	833	1077	1244	1036	1242	1200	922	722	711	586	550	533	391	430	522	439	489
36	1150	1800	1700	1650	1667	950	733	883	933	767	550	508	500	417	500	633	617	504
SUM	13601	11109	9866	10609	13738	14523	12463	11747	11427	10991	10710	10705	9375	7993	7485	7203	6762	6771
Sx SIN	-1186	-2874	-4169	-6085	-9714	-11901	-11295	-11346	-11334	-10949	-10345	-9702	-7680	-5652	-4293	-3046	-1750	-590

DEFLECTION STATION #1

DEFLECTION RESULTS RICE RINGS 22-29

Complete Bouguer Anomaly Component

	22	23	24	25	26	27	28	29
1	34	33	33	32	31	79	75	73
2	34	34	33	33	32	30	76	76
3	35	34	34	33	33	32	73	79
4	35	35	35	34	34	33	81	82
5	36	36	35	35	35	35	33	33
6	37	37	37	37	36	36	34	36
7	33	33	33	33	33	33	36	33
8	38	39	39	39	38	39	88	91
9	39	39	39	40	40	42	40	44
10	39	40	40	42	43	45	44	43
11	40	41	42	43	46	48	49	102
12	41	42	43	45	47	100	102	103
13	41	43	45	46	48	101	103	105
14	42	44	45	47	49	102	105	107
15	42	44	45	47	100	102	106	107
16	42	44	45	48	100	102	107	107
17	42	44	45	47	100	101	107	107
18	42	43	45	46	49	100	106	105
19	41	42	44	45	47	49	101	103
20	40	41	43	44	45	48	49	101
21	40	40	41	42	44	45	47	43
22	39	40	40	40	42	43	44	45
23	39	39	39	39	39	40	41	42
24	33	33	33	39	39	39	39	39
25	33	33	33	33	33	37	37	37
26	37	37	37	37	36	36	36	36
27	36	36	36	35	35	35	35	34
28	36	35	35	34	33	33	32	30
29	35	34	34	33	32	81	79	77
30	34	34	33	32	31	79	77	75
31	34	33	33	31	30	73	75	73
32	34	33	32	31	79	77	74	70
33	34	33	32	31	79	76	73	69
34	33	33	32	31	79	76	73	63
35	33	33	32	31	30	76	73	69
36	34	33	32	31	30	77	75	70

Table 11 (cont.)
DEFLECTION STATION #1

page 22

DEFLECTION RESULTS RICE RINGS 30-36

Complete Bouguer Anomaly Component

	30	31	32	33	34	35	36	Sum X Sine
1	69	63	62	57	55	51	43	91.56
2	73	70	66	64	59	56	54	- 282.09
3	76	75	73	72	70	64	53	507.22
4	31	79	77	73	75	74	66	637.74
5	33	82	81	31	31	30	75	877.51
6	36	35	35	34	34	33	30	1046.12
7	38	38	33	33	37	37	37	1191.79
8	91	92	92	93	90	91	94	1308.80
9	96	97	97	96	97	93	102	1400.66
10	101	102	102	102	103	105	111	1461.43
11	103	105	106	107	110	113	115	1468.17
12	105	103	111	113	113	116	119	1412.02
13	103	111	113	115	117	120	125	1303.35
14	110	113	115	117	121	126	133	1253.65
15	111	114	116	119	124	123	133	942.43
16	110	114	117	119	124	123	137	727.63
17	110	113	116	113	123	123	134	423.14
18	103	112	114	117	120	126	130	140.65
19	106	109	112	114	117	122	126	- 137.60
20	103	106	109	111	114	119	123	- 400.11
21	101	103	105	98	111	115	113	- 663.02
22	93	100	102	105	107	113	114	- 844.34
23	93	95	96	99	103	105	109	- 1093.28
24	39	90	91	93	95	97	99	- 1116.57
25	37	37	36	36	37	90	93	- 1193.60
26	85	34	33	32	30	30	31	- 1223.80
27	32	30	73	74	72	69	69	- 1201.42
28	77	75	73	70	65	63	57	- 1143.64
29	75	73	69	65	63	56	43	- 1066.35
30	73	63	65	63	60	51	44	- 963.84
31	69	66	64	60	54	43	42	- 851.97
32	67	65	62	56	52	45	41	- 785.88
33	66	64	60	54	49	44	40	- 575.89
34	66	64	57	53	43	44	40	- 441.27
35	66	64	57	54	49	46	42	- 260.09
36	67	64	53	55	52	43	45	- 89.03

Table 12

DEFLECTION STATION #2

page 23

DEFLECTION RESULTS RICE RINGS 22-29

Complete Bouguer Anomaly Component

	22	23	24	25	26	27	28	29
1	96	95	94	93	91	90	89	37
2	96	95	94	93	92	91	89	33
3	97	94	94	94	93	92	90	39
4	97	95	95	94	93	93	91	90
5	98	97	97	95	95	94	93	92
6	93	97	97	97	97	96	94	94
7	99	93	93	93	93	93	93	97
8	100	99	99	99	99	99	100	100
9	101	101	101	101	101	101	102	103
10	102	102	103	103	103	103	104	106
11	103	103	104	104	104	105	106	109
12	104	104	105	105	106	107	109	110
13	104	105	106	107	107	109	111	112
14	105	106	107	108	109	111	112	113
15	105	106	107	109	110	111	113	114
16	106	107	108	109	111	112	113	114
17	106	107	108	110	111	112	114	115
18	106	107	108	110	111	112	113	115
19	106	107	108	110	111	112	113	114
20	106	106	108	109	110	112	113	114
21	105	106	107	108	109	111	112	113
22	105	106	106	107	108	109	111	112
23	104	105	105	106	106	108	109	110
24	104	104	105	105	105	105	106	106
25	103	103	104	103	103	103	103	103
26	102	102	102	102	102	102	101	101
27	102	102	101	101	101	100	99	96
28	101	101	101	100	99	96	95	92
29	100	100	100	99	96	94	92	90
30	100	99	97	96	94	92	90	88
31	99	98	95	94	93	91	89	37
32	98	97	95	93	92	90	88	36
33	97	96	94	93	91	89	88	36
34	96	95	94	93	91	89	88	36
35	96	95	94	92	91	89	88	36
36	96	95	94	93	91	90	88	37

Table 12 (cont.)
DEFLECTION STATION #2

page 24

DEFLECTION RESULTS RICE RINGS 30-36

Component Bouguer Anomaly Component

	30	31	32	33	34	35	36	Sum X	Sine
1	36	34	33	31	76	69	64	111.44	
2	37	35	34	32	77	76	75	337.43	
3	33	37	35	33	79	31	31	560.79	
4	39	39	38	36	32	35	34	774.92	
5	91	90	90	90	38	37	33	979.33	
6	94	94	94	94	92	90	92	1163.26	
7	97	93	93	93	93	96	93	1329.54	
8	100	102	105	105	106	106	110	1476.36	
9	105	107	110	112	113	115	123	1589.94	
10	103	111	113	115	117	122	129	1634.76	
11	110	112	114	117	121	125	132	1612.09	
12	112	114	116	119	123	123	135	1537.99	
13	113	115	117	120	125	131	139	1409.84	
14	114	116	119	122	127	135	146	1237.43	
15	115	113	120	125	132	142	153	1021.01	
16	116	119	123	123	135	144	160	762.79	
17	117	120	125	123	135	145	160	469.20	
18	117	120	125	123	133	143	153	157.05	
19	116	120	123	126	129	136	146	- 154.95	
20	116	113	120	123	126	130	136	- 452.12	
21	115	116	113	119	122	125	129	- 724.76	
22	113	115	116	117	117	113	123	- 965.37	
23	111	112	112	113	113	113	115	- 1160.35	
24	106	107	107	107	106	107	107	- 1300.07	
25	103	102	102	101	100	99	100	- 1388.45	
26	100	97	96	93	92	90	33	- 1419.87	
27	95	92	90	89	33	36	31	- 1416.60	
28	90	39	36	34	32	76	72	- 1358.81	
29	33	36	33	31	75	70	63	- 1275.95	
30	86	34	31	76	63	65	60	- 1156.44	
31	35	33	77	71	65	59	53	- 1014.99	
32	34	31	76	69	63	56	50	- 861.25	
33	34	31	76	70	62	56	50	- 695.78	
34	34	31	77	73	66	53	52	- 516.84	
35	35	82	30	75	71	60	55	- 320.65	
36	35	33	32	79	75	65	56	- 109.78	

Table 13
DEFLECTION STATION #3

page 25

DEFLECTION RESULTS RICE RINGS 22-29
Complete Bouguer Anomaly Component

	22	23	24	25	26	27	28	29
1	120	113	116	115	113	110	105	102
2	120	120	113	116	115	112	111	106
3	121	121	120	113	113	114	113	111
4	122	122	122	121	120	117	115	113
5	123	123	123	123	122	121	119	116
6	125	125	125	125	125	125	123	121
7	126	126	127	127	123	123	123	127
8	127	123	129	130	131	131	131	131
9	127	129	130	131	131	133	133	134
10	123	129	131	131	132	133	135	136
11	129	130	131	131	133	134	136	133
12	129	130	131	131	133	135	137	140
13	129	129	131	131	133	135	133	140
14	129	129	130	131	132	135	133	140
15	129	129	129	130	132	134	137	140
16	123	129	129	130	131	133	135	133
17	127	123	129	129	129	132	134	136
18	127	127	123	129	129	130	132	133
19	127	127	127	123	123	129	129	131
20	126	126	126	127	127	123	128	129
21	125	125	125	125	125	123	127	127
22	124	124	124	124	124	124	124	125
23	123	123	123	123	123	123	123	122
24	122	122	122	122	121	121	121	120
25	122	121	121	120	120	119	119	113
26	121	121	120	119	113	117	116	115
27	121	120	119	113	116	115	115	114
28	120	119	117	116	115	114	113	112
29	119	113	116	115	114	113	112	110
30	113	116	115	114	113	111	110	107
31	117	116	115	113	111	109	107	105
32	117	115	114	112	110	103	106	103
33	117	115	114	111	109	107	104	100
34	117	116	114	111	109	106	102	99
35	113	116	115	112	110	107	101	99
36	119	117	115	113	111	103	103	99

Table 13 (cont.)
DEFLECTION STATION #3

page 26

DEFLECTION RESULTS RICE RINGS 30-37

Complete Bouguer Anomaly Component

	30	31	32	33	34	35	36	Sum X Sine
1	101	100	98	94	90	87	33	- 135.33
2	103	102	98	95	92	88	35	409.16
3	105	103	99	97	93	89	36	679.54
4	112	106	102	98	95	92	88	943.57
5	114	112	106	102	98	95	92	1194.29
6	113	115	112	107	104	100	97	1431.14
7	125	122	117	114	111	107	104	1733.28
8	131	130	127	123	119	116	113	1832.31
9	135	135	135	133	130	126	124	1958.53
10	137	139	140	140	138	133	136	2015.31
11	140	141	143	147	143	150	152	2011.97
12	141	144	145	153	155	159	162	1925.89
13	142	145	147	157	161	165	170	1763.74
14	142	145	147	159	165	170	175	1532.29
15	142	144	146	159	167	173	179	1244.71
16	141	143	145	157	165	173	180	911.55
17	140	142	144	155	162	171	181	553.57
18	136	139	142	150	157	170	181	183.99
19	133	136	140	145	153	165	178	- 176.67
20	130	133	136	139	146	157	171	- 525.11
21	128	129	131	136	140	149	162	- 836.75
22	126	126	128	129	134	142	147	- 1104.18
23	122	122	123	123	125	132	140	- 1322.98
24	120	119	113	119	120	124	127	- 1489.31
25	117	116	116	116	116	117	120	- 1611.40
26	115	114	113	113	113	113	113	- 1601.63
27	113	112	110	107	106	105	105	- 1689.56
28	111	110	106	103	99	98	96	- 1642.73
29	109	106	91	97	94	92	88	- 1539.65
30	105	103	83	94	90	83	35	- 1411.11
31	103	100	86	93	89	35	33	- 1255.01
32	100	97	84	91	86	81	77	- 1061.36
33	98	95	90	88	85	84	79	- 853.11
34	97	94	91	88	87	85	82	- 633.06
35	97	95	93	90	88	85	83	- 390.53
36	93	97	95	92	89	86	32	- 132.89

Table 14

DEFLECTION STATION 2
BOUGUER CORRECTION COMPONENT
RICE RINGS 15-21

	15	16	17	18	19	20	21	SUM	SUM X SIN
1	720	720	770	800	748	730	695	5133	452
2	730	710	750	750	723	725	690	5083	1315
3	750	700	720	750	770	750	730	5170	2105
4	760	720	700	740	776	770	755	5221	2995
5	760	730	720	720	770	742	700	5142	3636
6	740	730	730	690	715	725	662	5042	4130
7	740	700	700	660	652	672	640	4764	4313
8	720	710	750	700	670	740	633	4823	4663
9	750	750	800	750	725	650	625	5060	5041
10	770	750	750	650	663	640	605	4843	4325
11	730	710	650	600	635	642	610	4627	4469
12	670	650	650	660	700	625	655	4680	4241
13	670	650	670	750	770	715	690	4915	4026
14	670	630	700	700	750	732	742	4974	3517
15	700	740	720	730	730	765	775	5160	2960
16	720	770	790	800	800	730	803	5463	2311
17	640	770	800	850	860	832	900	5702	1476
18	650	750	750	800	865	950	950	5715	498
19	630	750	750	760	782	832	812	5366	-463
20	700	700	750	750	762	750	782	5104	-1344
21	730	700	740	800	830	820	900	5670	-2326
22	760	750	730	730	730	840	903	5543	-3182

Table 14 (cont.)

DEFLECTION STATION 2

BOUGUER CORRECTION COMPONENT

RICE RINGS 15-21

	15	16	17	18	19	20	21	SUM	SUM X SIN
23	730	310	760	760	790	343	225	5673	-4011
24	730	320	340	760	755	730	368	5603	-4590
25	730	760	360	330	755	792	912	5639	-5111
26	770	750	750	310	330	770	325	5505	-5317
27	790	300	300	300	790	735	340	5605	-5504
28	320	340	350	350	370	742	363	5340	-5313
29	330	350	350	350	330	345	335	5390	-5609
30	350	360	300	340	315	352	303	5325	-5279
31	350	700	760	350	320	760	740	5570	-4563
32	340	760	750	800	858	775	730	5513	-3898
33	310	770	740	810	310	760	735	5485	-3146
34	780	730	750	340	810	760	758	5423	-2294
35	740	730	750	310	300	780	760	5378	-1392
36	730	725	760	330	365	750	745	5405	-471